ESTIMATING SOURCE TERM FOR GROUND-WATER CONTAMINATION

by

Michael LeFrancois

A thesis submitted to the Faculty and Board of Trustees of the Colorado School of Mines in partial fulfillment of the requirements for the degree of Master of Science (Geological Engineering).

Golden, Colorado

Date: _____

Signed: _____
Michael LeFrancois

Approved: _____
Dr. Eileen Poeter
Thesis Advisor

Golden, Colorado

Date: _____

_____
Dr. John Humphrey
Acting Department Head
Department of Geology and
Geological Engineering

ABSTRACT

In this study, nonlinear regression has been used to estimate the time and magnitude of Trichloroethylene (TCE) that entered the ground-water system in the Bunker Hill Ground-Water Basin of San Bernardino County, California. This study relies on 54 years of hydraulic head and stream flow observations and 24 years of contaminant concentrations throughout the aquifer. Contaminant observations include censored data, i.e., measurements below the detection limit. A new approach (the censored-residual approach) for using censored data is implemented, in which the detection limit is used as the observed value to calculate the residual (difference between observed and simulated values) when the simulated value exceeds the detection limit, and a residual of zero is used when the simulated value is below the detection limit. A synthetic example demonstrates that the censored-residual approach produces better estimates of the source term, thus it is used to calibrate a model of a TCE plume in the Bunker Hill Basin. Alternative conceptual models are calibrated in order to evaluate uncertainty associated with the source term. In conjunction, Akaike's Information Criterion is used to calculate model weights and average the results. Given the current conceptual model, the available data, and this limited analysis, we have not determined when the bulk of the mass reached the water table. Future work, involving evaluation of alternative conceptual models and further analysis of the field data, is suggested to facilitate that determination.

TABLE OF CONTENTS

LIST OF FIGURES

LIST OF TABLES

ACKNOWLEDGMENTS

I would like to express gratitude to my advisor, Dr. Eileen Poeter, who always was able to provide guidance, support, suggestions, and keep me in touch with reality no matter how many directions she was pulled due to her tremendous amount of obligations. I thank my colleague, John Anthony for his continuous input, recommendations, and knowledge provided during the course of this work. Finally, I also thank my committee members Paul Santi, Michael Gooseff, and Dennis Helsel for their advice and contributions during the course of the project.

CHAPTER 1: OVERVIEW

Introduction

A plume of Trichloroethylene (TCE) exists in the Bunker Hill Ground-Water Basin. The basin covers an area of approximately 120 square miles and is located in San Bernardino County, about 60 miles northeast of Los Angeles, California (Figure 1.1). The specific conditions related to the magnitude and timing of TCE releases are unknown due to limited operational records, but its location is believed to be a former industrial facility (Figure 1.2). Observations of water levels, stream-flow rates, and TCE concentrations in ground water are used to estimate the contaminant source term (mass and timing) with respect to its arrival at the water table. The time of transport through the vadose zone must be subtracted from the time of arrival at the water table in order to estimate the time when contaminants are introduced at the ground surface.

An existing flow model of the basin (Danskin, 2006) is modified to facilitate the contaminant transport modeling. Data for calibration includes 54 years of water levels and stream flows, and 24 years of concentration measurements from ground-water monitoring by local and governmental agencies.

The goal of this project is to use the available data to estimate the time when TCE reached the ground water using nonlinear regression and model averaging. Results of this research are presented in Chapters 4 and 5. Chapter 2 describes the Bunker Hill

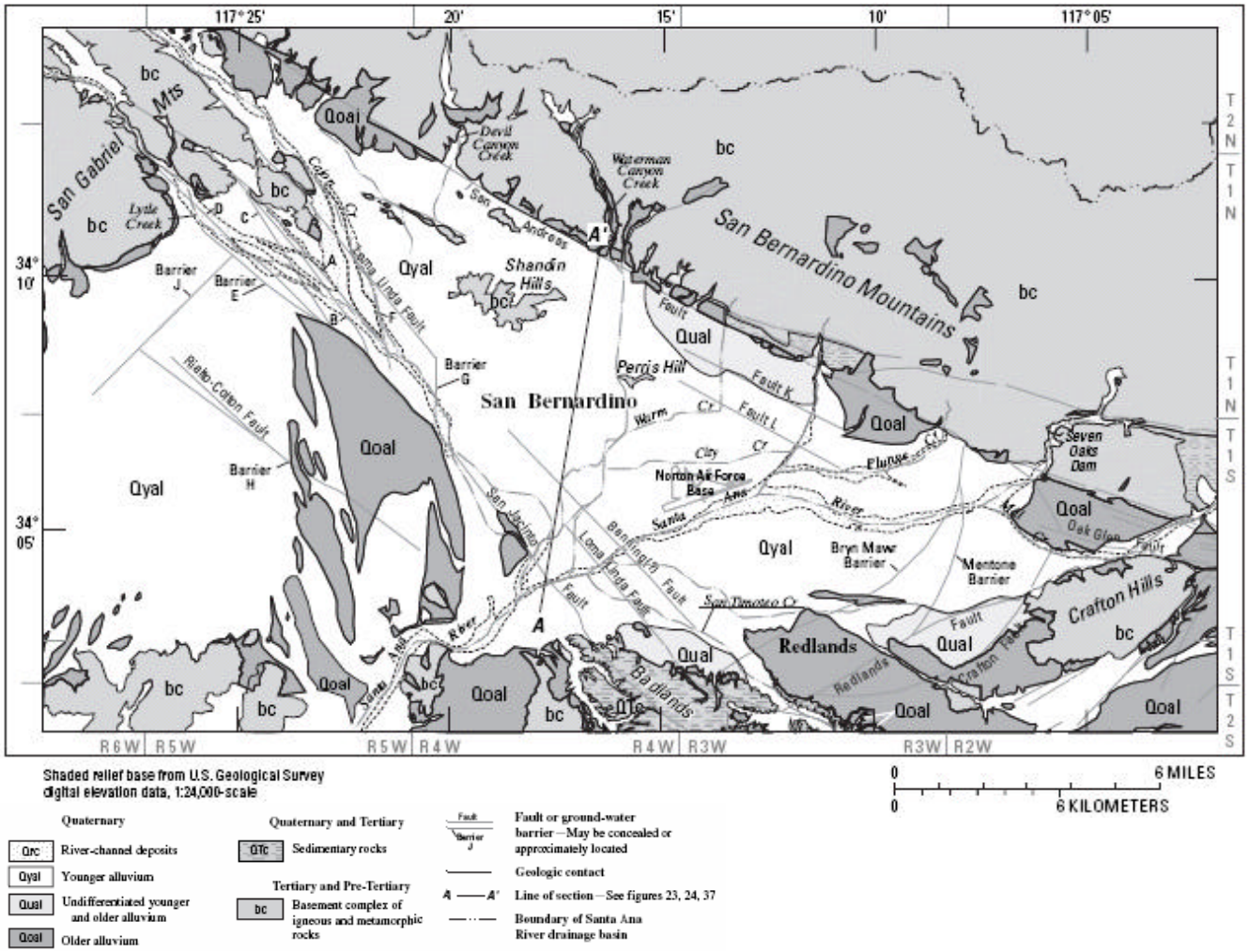

Figure 1.1: Geographic setting and generalized geology of the Bunker Hill Ground-Water Basin, from Danskin (2006).

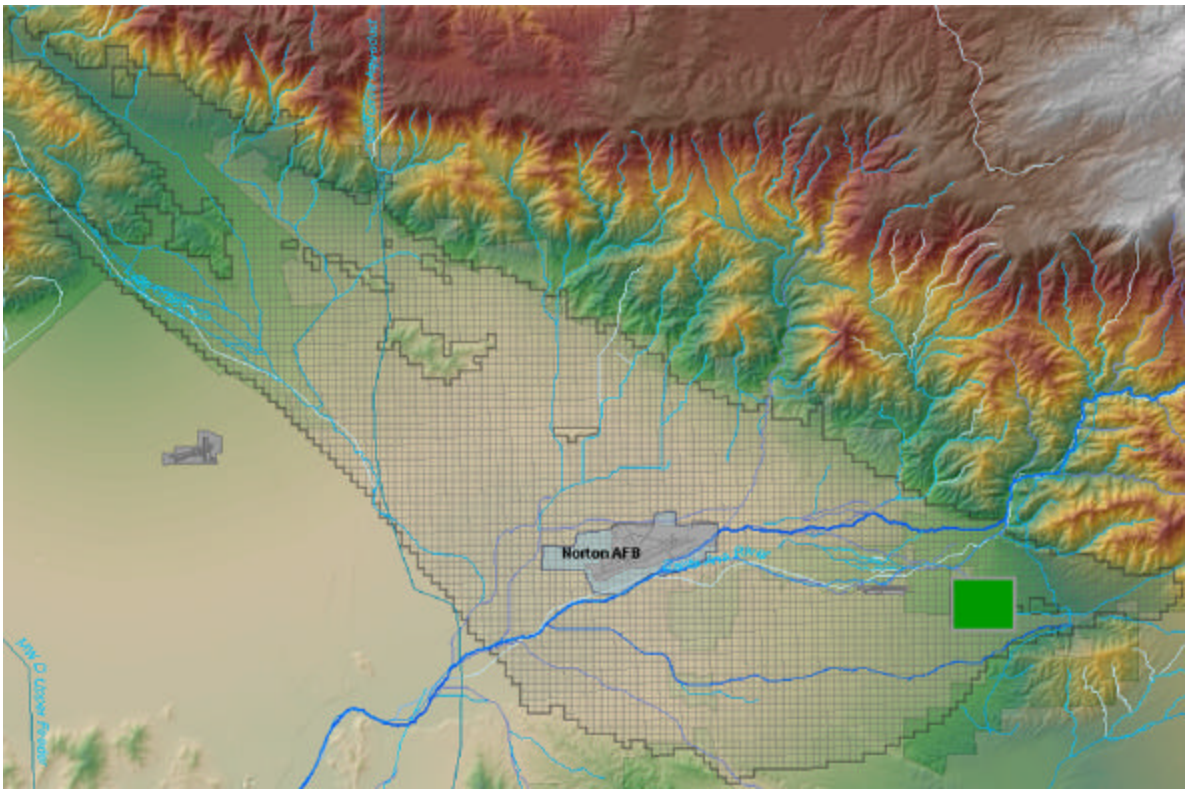

Figure 1.2: Finite-Difference grid and assumed source of TCE (represented by the green rectangle).

Ground-Water Basin, and Chapter 3 delineates the flow and transport model of the basin. Given that background, Chapter 4 describes the use of censored values for model calibration using both synthetic examples and the TCE plume in the Bunker Hill Basin. Chapter 5 details the results of regression and model averaging with various prescribed source functions to estimate the character of the source distribution for the TCE plume. The main findings are highlighted in Chapter 6.

Two issues related to estimating the contaminant source term are addressed in this work: 1) inclusion of observations that are below the detection limit of laboratory

analysis (these are also known as 'censored' data); and 2) evaluation of multiple conceptual models of the source. To use censored data, we set residuals to zero if the simulated value is less than detection limit (indicating a perfect fit to the observation), otherwise we calculate the residual as the detection limit minus the simulated value. Biased results may occur because these observations can only produce zero or negative residuals, but this is tolerated in order to accommodate all the information in the parameter estimation process. Provided a significant number of observations are above the detection limit, then the use of all the observations produces a more realistic representation of the system. The second issue, consideration of multiple conceptual models of the source is important because generally, data describing the character of the source are not available, so the conceptual model of the source is uncertain. The conceptual model will influence the mass and timing estimated when calibrating the advection-dispersion equation, therefore various conceptual models should be considered. Although a best-fit model can be identified, it may not be the best representation of the source given the sparse, uncertain observations and model. Hence, multiple models need to be considered and their results should be averaged. Previous work related to use of censored data and consideration of multiple models is discussed in the following section.

Previous Work

Often, censored data are present in data collected during social sciences, economics, medical, and industrial research (Helsel, 2005). Even though geohydrologists have been dealing with censored data for some time, their treatment in the calibration process has been less than satisfactory: ignoring the values; deleting them; making them null; or setting the values equal to some fraction of the detection limit (Helsel, 2005; Gilliom and Helsel, 1986). For instance, Helsel (2005) states, "a common approach is to substitute one-half the detection limit. However, this assumes a spike at one value for all nondetects, which is not a realistic assumption. The method for determining the detection limit among laboratories, and using a value that depends on the detection limit introduces an artificial signal that reflects laboratory conditions rather than concentration patterns in the aquifer."

One of the most detailed investigations of censored data was completed by Gilliom and Helsel (1986). They estimated the mean, standard deviation, median, and interquartile range for several assumptions regarding censored observations. They make these estimates for several cases, making different assumptions about the censored values, namely that they: are zero; are equal to the detection limit; have a uniform distribution between zero and the detection limit; have a distribution represented by the portion of a normal distribution between zero and the detection limit; or have a distribution represented by the portion of a lognormal distribution between zero and the

detection limit. They concluded that, for the purpose of estimated population statistics, the best approach is assuming censored observations follow the zero to detection-limit portion of a lognormal distribution. Further applications using censored data are discussed in Helsel (2005), which describes methodologies designed to analyze censored data.

The second issue addressed in this work regards evaluation of alternative conceptual models when estimating the source term. For the past 15 years various mathematical applications have been developed to evaluate the advective-dispersive equation in an inverse sense in order to gain insight into the history of contaminant release (Atmadja et al., 2001). One of the original studies used least-squares regression and linear programming (Gorelick et al., 1983) to estimate the source term. Wagner and Gorelick (1986) expanded that work. Other work coupled parameter estimation and contaminant source characterization (Wagner, 1992; Medina and Carrera, 1996). Several advances were made with nonlinear optimization for identification of pollution sources (Mahar and Datta, 2000), nonlinear least squares (Alapati and Kabala, 2000), Gauss-Newton inversion (Essaid et al., 2003), Levenberg-Marquardt optimization (Sonnenborg et al., 1996; Parker and Islam, 2000), and a simulation-regression management model involving three linked components: a flow and transport model combined with nonlinear regression; moment analysis; and nonlinear stochastic optimization (Wagner and Gorelick, 1987). Techniques for characterizing the source term incorporated Tikhonov regularization (Skaggs and Kabala, 1994; Liu and Ball, 1999; Neupauer et al., 2000),

quasi-reversibility (Skaggs and Kabala, 1995), Monte Carlo simulation (Skaggs and Kabala, 1998), and the backwards beam method (Atmadja and Bagtzoglou, 2001). Geostatistical approaches such as a Bayesian framework (Snodgrass and Kitanidis, 1997), and the adjoint method (Neupauer and Wilson, 1999, 2001, 2002, 2004; Michalak and Kitanidis, 2004) have also been used to determine the source term. Recent developments include the constrained, robust, least-squares method (Sun et al., 2006).

One of the first works to address conceptual model selection was Carrera and Neuman (1986) where they used information criteria to explore the estimation of aquifer parameters under transient and steady state conditions by revisiting the maximum likelihood method and incorporating prior information about model parameters. They concluded that maximum likelihood theory lends itself to the definition of model identification criteria that may be useful for selecting the best model. Later, Poeter and Anderson (2005) explained that the bias-corrected Akaike Information Criterion (AICc), which is rooted in the minimization of Kullback-Leibler mean information loss (a measure of the departure of the model from the true system), is the preferred criterion for weighting and averaging alternative models. Anderson (2003) pointed out the forgotten second order variant of AIC termed AICc, which is used for smaller sample sizes typical in ground-water modeling. Burnham and Anderson (2002) provide an in-depth discussion of model selection and multi-model analysis.

CHAPTER 2: DESCRIPTION OF THE BUNKER HILL GROUND-WATER BASIN

The Bunker Hill Basin is geologically complex with respect to geomorphic changes over geologic time. The basin boundaries are formed by regional-scale faults and topography such as the San Andreas Fault and the San Bernardino Mountains along the northern boundary, and the San Jacinto Fault along the southern boundary. Both the San Andreas and the San Jacinto Faults have been fairly well characterized (Dutcher and Garrett, 1963; Danskin, 2006). The Banning and Crafton Faults, as well as the Badlands and Crafton Hills form the southeastern boundary. The western boundary of the basin is delineated by the San Gabriel Mountains and the Loma Linda Fault (Figure 1.1). "Current geologic understanding suggests that the Bunker Hill basin is a pull-apart basin, i.e., a tectonic strike-slip basin which developed over the last 1.7 million years in response to a right step between the San Jacinto and San Andreas Faults." (SBVMWD, 2004).

The unconsolidated material that fills the basin includes river-channel deposits and alluvium, both of Holocene age, and older alluvium of Pleistocene age (Lowell et al., 1988). The alluvial material is water-bearing and consists of deposits of sand, gravel, and boulders interspersed with lenticular deposits of silt and clay, forming what is termed the "valley-fill aquifer." Previous investigations divided the valley-fill aquifer into six

hydrologic sub-units: 1) upper confining member; 2) upper water bearing member; 3) middle confining member; 4) middle water bearing; 5) lower confining member; and 6) lower water bearing (Dutcher and Garett, 1963). However, Hardt and Hutchinson (1980) combined the six hydrogeologic units into a two layer hydrostratigraphic model for simplification purposes with thicknesses varying from approximately 120 to more than 380 feet for each layer. The two layer designation is the basis of the recent USGS flow model developed by Danskin (2006).

Danskin (2006) suggests that, "Components of the water budget consist of natural and artificial recharge, ground-water inflow, ground-water pumping, return flow from pumping, evapotranspiration, and surface and subsurface outflow through the Colton-Narrows, where the Santa Ana River crosses the San Jacinto Fault." The largest recharge to the basin occurs from infiltration of stream-flow runoff from the San Gabriel and San Bernardino Mountains, primarily via seepage through stream/river beds. Specifically, three main tributary streams contribute more than 60 percent of the total recharge to the ground-water system: the Santa Ana River, Mill Creek, and Lytle Creek. Lesser contributors include: Canyon Creek, Plunge Creek, and San Timoteo Creek. Other sources of recharge include seepage of imported water from artificial basins, local runoff, return flow from groundwater flow from adjacent areas, and precipitation falling directly on the basin, which is assumed negligible due to the semiarid climate (Danskin, 2006). Recharge also occurs as groundwater flow across both the Crafton fault and the Badlands (Danskin, 2006; Lowell et al., 1988). Sources of discharge are groundwater out flow,

evapotranspiration, and ground-water pumping (Danskin, 2006). Groundwater outflow occurs across a designated ground-water barrier, Barrier E, where Lytle Creek emerges from the San Gabriel Mountains in the western section of the basin and at the Colton-Narrows (Danskin, 2006). Evapotranspiration occurs throughout the basin.

Most ground water leaves the basin via pumping and evapotranspiration. Of the remaining ground water, most exits at Colton-Narrows, which is also the surface water discharge location, while a lesser amount exits through Barrier E.

For further details, Danskin (2006), Dutcher and Garrett (1963), Hardt and Hutchinson (1980), and Lowell et al., (1988) provide descriptions of the physiography and hydrology of the basin.

CHAPTER 3: FLOW AND TRANSPORT MODEL DEVELOPMENT

Flow Model

Danskin's (2006) flow model of the Bunker Hill Basin is used as a basis for the work presented herein. Danskin used MODFLOW-96 (Harbaugh et al., 1996). However, Danskin modified the source code of MODFLOW-96 to represent site-specific boundary conditions of the Bunker Hill Basin which entailed adding specialized internal source/sink packages. For ease of use, the Danskin model is updated to MODFLOW-2000 (Harbaugh et al., 2000), and modified for analysis with automated regression.

Danskin's conceptual model of ground-water flow in the valley-fill aquifer includes an upper unconfined model layer and a lower, confined model layer with transmissivities based on Hardt and Hutchinson (1980). Hardt and Hutchinson (1980) estimated transmissivity using specific capacity tests performed by the California Department of Water Resources (Eckis, 1934). These transmissivity values are converted to hydraulic conductivities by obtaining the elevation of the top and bottom of each layer and dividing the transmissivities by the layer thicknesses. The derivation of layer elevations entailed digitizing elevation values for each grid cell of the respective model layer provided by figures in Appendix B of the draft EIR report (2004). Specific yield values provided by Eckis (1934) for the top layer were digitized and interpolated to each cell location (Danskin, 2006). Storativity for layer two is set at 0.0001 to represent a confined aquifer

(Danskin, 2006; EIR, 2004). Vertical leakance between layers is based on estimates of Hardt and Hutchinson (1980). The time period for flow simulation begins on January 1, 1945 and continues for 60 years ending December 31, 2004. Transient simulations in MODFLOW are divided into stress periods during which stresses, such as pumping and stream influx vary. This model has 60 one-year long stress periods with each annual stress period subdivided into 10 time steps and a multiplier of 1.2. The grid domain includes the entire basin with 184 columns in the x-direction and 118 rows in the y-direction. Cell dimensions are a uniform 820 feet (250 meters) in both the x and y directions, where each model cell covers about 15 acres of land (Figure 1.2). The ground-water flow equation is solved using the Preconditioned Conjugate Gradient solver package, with convergence tolerance of 0.01 ft on heads and residuals, a maximum of 2000 iterations, and a relaxation factor of 0.97.

Boundary Conditions of the Danskin Model

The hydrologic boundaries (Figure 3.1) for Danskin's model are specified flux around the perimeter of the upper layer except at the convergence of all surface water features in the basin known as the Colton-Narrows located along the San Jacinto Fault, which is represented by a specialized head dependent flux. Flow from Colton-Narrows uses simulated water levels at the Heap Well location to calculate discharge (Danskin 2006). The flux is zero along the remaining portions of the San Jacinto Fault completing the southern boundary of the upper layer. The lower layer is surrounded by a no flow boundary except at specified flux boundaries in the northwest portion of the basin within the San Gabriel Mountains and upper Lytle Creek area, southern portions within the Badlands, and southeastern portions within the Crafton Hills area. Specified flux boundaries represent ground-water inflow, faults are represented via horizontal flow barriers in MODFLOW, streams and rivers are represented with a head dependent flux boundary that allows stream stage to change in response to flow between the ground and surface water systems, and pumping is simulated as specified fluxes in the central locations of the basin.

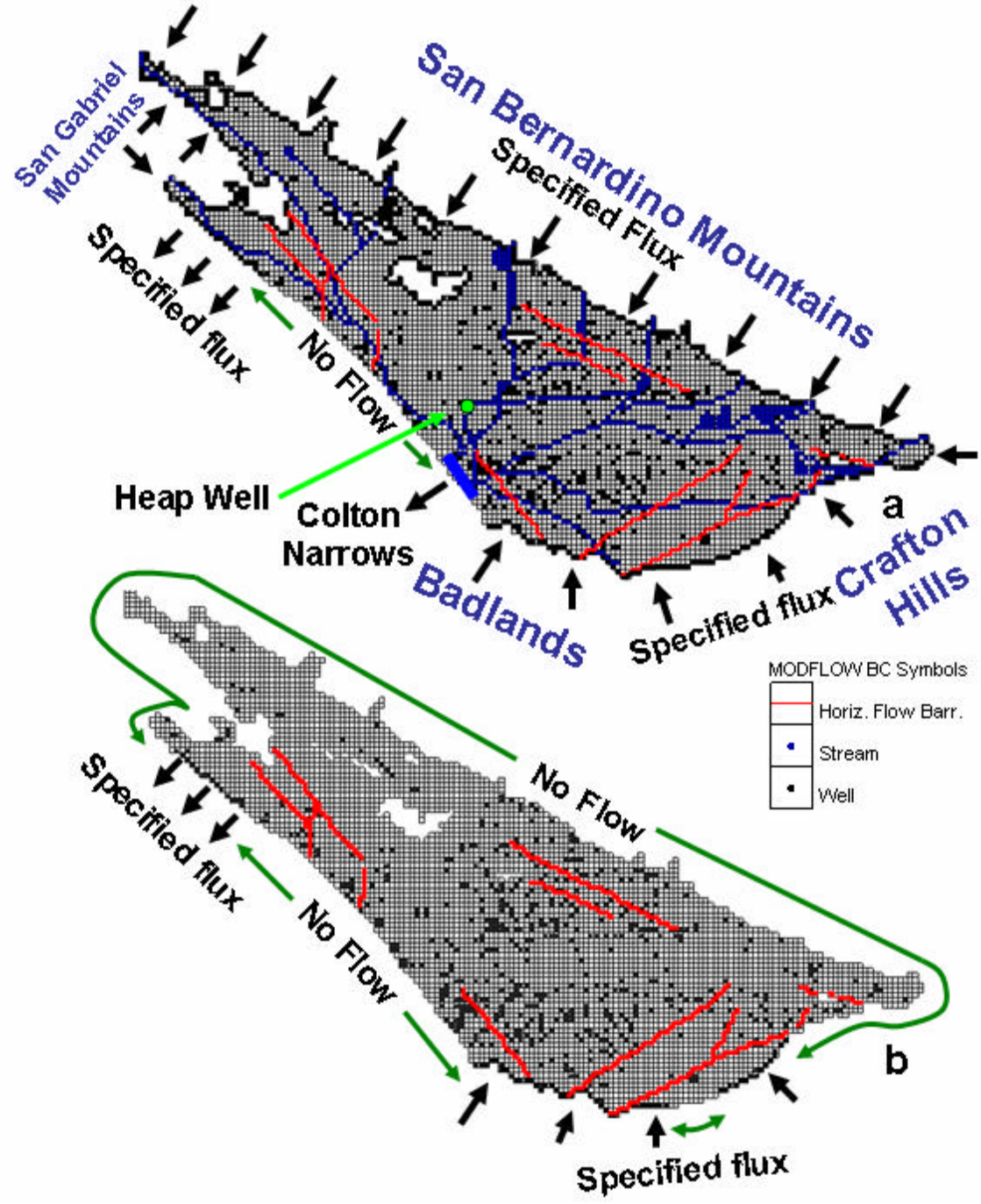

Figure 3.1: Danksin boundary conditions a) the upper and b) lower (bottom) layers of the Bunker Hill ground-water flow model.

Modified Boundary Conditions

The boundary conditions (Figure 3.2) are unchanged in the modified model except for the outflow at Colton-Narrows, the inflow across the Crafton Fault (both were changed to a standard general head boundary), and flux added to the Zanja ditch (discussed later).

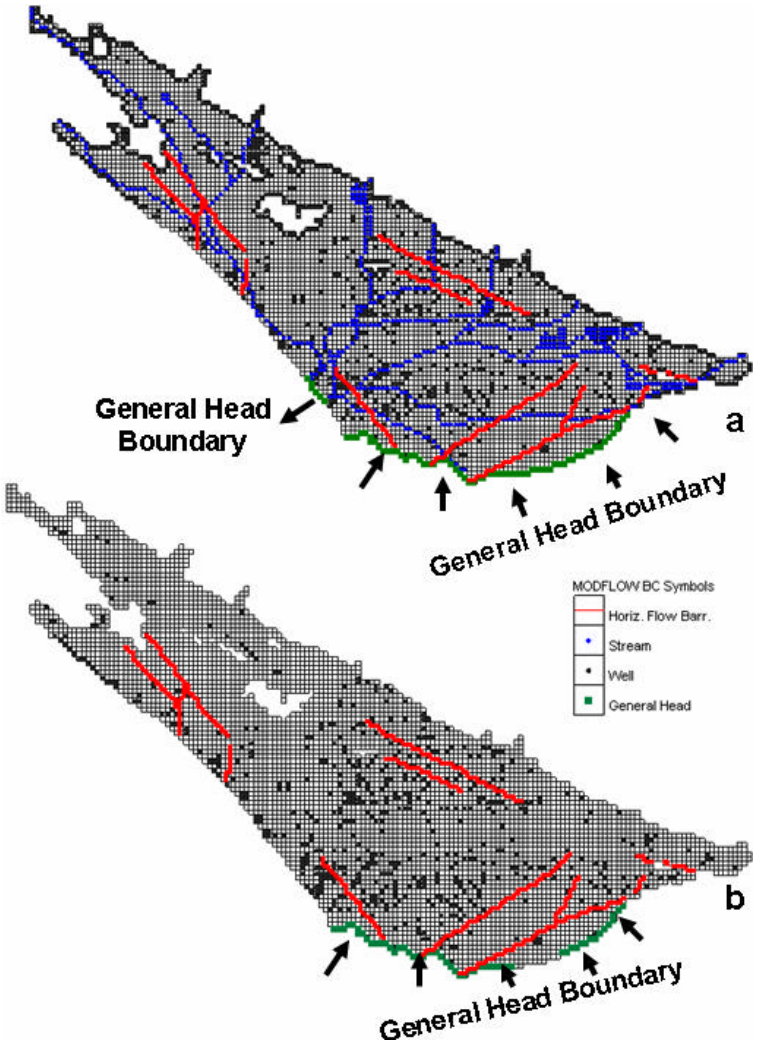

Figure 3.2: Altered boundary conditions for the modified model: a) the upper and b) lower (bottom) layers of the Bunker Hill ground-water flow model.

The boundary conditions, recharge/discharge fluxes in the modified flow model, and associated MODFLOW packages are listed in Table 3.1.

Table 3.1: Boundary conditions and associated MODFLOW packages.

	Recharge and Discharge Flux for the Modified Model	MODFLOW PACKAGE
Recharge	Gaged stream flow	STR
	Recharge from ungaged mountain front runoff	WEL
	Infiltration from direct precipitation	RCH
	Recharge from local runoff	RCH
	Return flow from pumping	WEL
	Imported water (artificial recharge)	WEL
	Southeasten boundary inflow	GHB
Discharge	Ground-water pumping	WEL
	Evapotranspiration	EVT
	Gaged stream flow	STR
	Groundwater flow	WEL
	Flow out of the Colton-Narrows	GHB

Transport Model

The modular three-dimensional transport and multi-species computer code MT3DMS (Zheng and Wang, 2005) is used to simulate TCE movement in the Bunker Hill Basin. The solute transport model requires the ground-water flux at each cell face so this information is saved for every stress period of the flow simulation. Also, several values of chemical and physical parameters are needed to construct the transport model and are discussed below, including retardation (which depends on the sorption distribution coefficient of TCE), bulk density and effective porosity of the aquifer, as well as the longitudinal, transverse, and vertical dispersivities. MT3DMS uses the same time discretization as the flow model to define the velocities. However, MT3DMS automatically calculates smaller time steps for simulation of dispersion in order to maintain a stable, accurate solution.

Physical and Chemical Properties

Retardation describes the velocity of a contaminant relative to ground water due to sorption of the contaminant to the aquifer matrix. Assuming a linear equation for sorption, the retardation coefficient is calculated as:

$$R = \frac{U}{v_c} = 1 + \frac{r_b}{f} k_d \; ; \; k_d = f_{oc} k_{oc} \qquad (3.1)$$

where, U is the ground-water flow velocity [L/t], V_c is the average velocity of a migrating contaminant [L/t], r_b is the dry bulk density of the aquifer [M/L^3], f is its effective porosity [-], k_d is the sorption distribution coefficient for the compound of interest (assumed to be linear for this project) [L^3/M], f_{oc} is the fraction of organic carbon [-], and k_{oc} is the partition coefficient between the contaminant and the natural organic matter [L^3/M]. For the sandy, loamy valley-fill aquifer a typical bulk density of 1.77 kg/L is estimated based on values for similar materials in the literature (USDA, 1996). The effective porosity is assigned values of specific yield determined by Eckis (1934). The fraction of organic carbon is site specific and is known to be small at this site (HSI, 1998; EIR, 2004), and retardation and distribution coefficient have not been measured. Consequently, a value of retardation is chosen based on information provided by HSI (1998), EIR (2004), and Montgomery and Welkom (1990). Parameter values are summarized (Table 3.2).

Longitudinal dispersivity is estimated by regression for each of the conceptual models describing the source functions discussed in Chapter 5. Prior estimates of dispersivity range from 100 ft (HSI, 1998) to 300 ft (EIR, 2004). Transverse dispersivity is set at one-third the value calculated for longitudinal and vertical dispersivity is one-hundredth of that value where both are based on field maps and cross-sections depicting the TCE contaminant plume.

Table 3.2: Summary of chemical and physical transport parameters, Note: [1]USDA, 1996, [2]Montgomery and Welkom, 1990.

Parameter	Units	Value
[1]Bulk Density, r_b	[kg/L]	1.77
Sorption Distribution Coefficient, k_d	[L/kg]	0.0214
Fraction Organic Carbon, f_{oc}	[--]	0.0002
[2]Distribution Coefficient, k_{oc}	[L/kg]	107

Peclet Number

The transport model uses the same grid design as the flow model. The Peclet number is the ratio of the cell length divided by dispersivity, and should be less than or equal to 2 to keep numerical dispersion small (Zheng and Bennet, 2002). The dispersivities estimated by regression for the alternative source functions are associated with Peclet numbers that are less than, equal to, or slightly larger than 2 (Chapter 5).

TCE contamination is simulated as a mass-loading using the source-sink mixing package of MT3DMS. A computer program is developed to generate the source-sink mixing file for each conceptual source function and is discussed in the appendix with further information provided on the CD included with this report.

The advective portion of the transport equation is solved using the third-order total-variation-diminishing (TVD) scheme, ULTIMATE. According to Zheng and Wang (2005), "The ULTIMATE scheme is mass conservative, without excessive numerical dispersion, is essentially oscillation-free, and superior to other solution methods." The

Courant number, which limits the time step size to maintain the distance that a solute advects in one time step, is specified as 0.5. This is generally required to be less than or equal to one to obtain an accurate solution (Zheng and Bennet, 2002). The Generalized Conjugate Gradient Solver (GCG) is used with a concentration change criteria for closure set at $1x10^{-4}$.

Evaluation of Flow Model for Transport Modeling

Assuming reasonable values of transport parameters, the Danskin (2006) flow model simulated the contaminant plume south of the observed location of the plume in the field (Figure 3.3). Proper simulation of the plume location cannot be achieved by adjusting transport parameters alone, because it requires adjustment of the flow direction. Thus, the Danskin flow model is recalibrated as discussed in the model calibration section of this chapter.

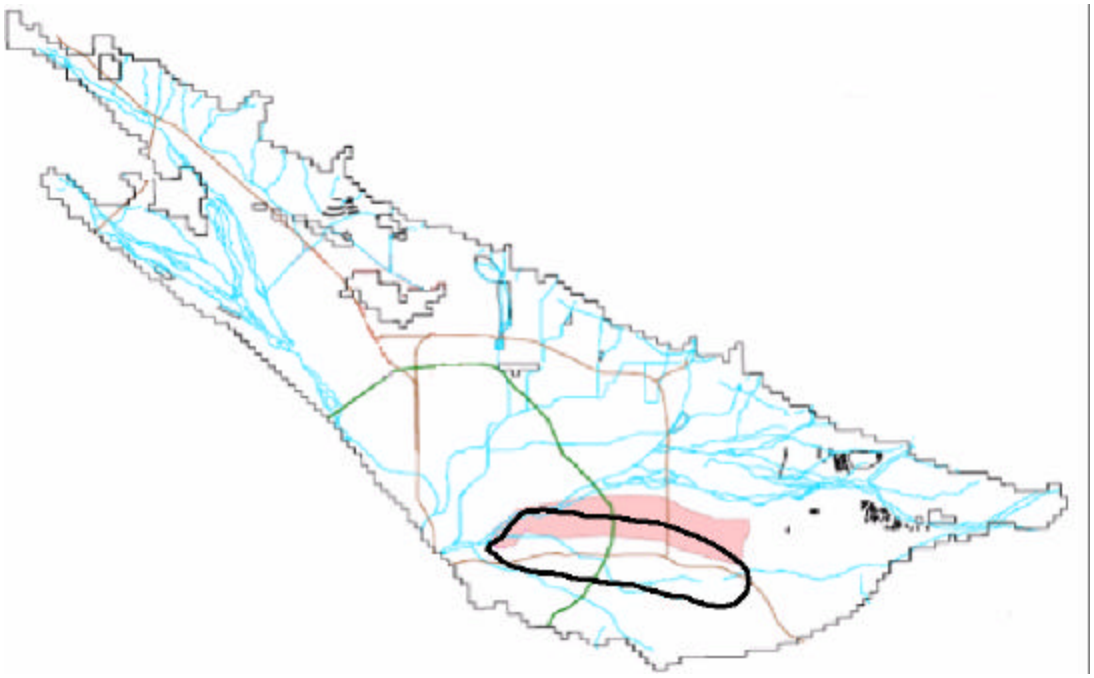

Figure 3.3: The simulated TCE plume location from Danskin's flow model is outlined in black. The underlying pink shaded region outlines the location of measured concentrations greater than 5 Parts-Per Billion (ppb) (EIR, 2004).

Parameter Estimation

UCODE_2005 Parameter Estimation Code

UCODE_2005 (Poeter et al., 2005) is used to perform inverse modeling by nonlinear regression with the purpose of estimating optimal values for selected parameters in order to minimize the squared weighted residuals between observations and simulated values. UCODE_2005 uses a modified Gauss-Newton approach to nonlinear regression with a weighted Least-Squares Objective Function (LSOF), (Hill, 1998):

$$S(b)=\sum_{i=1}^{ND} w_i[y_i - y_i^{'}(b)]^2+\sum_{p=1}^{NPR} w_p[p_p - p_p^{'}(b)]^2 \qquad (3.2)$$

where:

b	is a vector containing values of each of the NP parameters being estimated;
ND	is the number of observations;
NPR	is the number of prior information values;
$y_{i,}$	is the i^{th} observation being matched by the regression;
$y_i'(b)$	is the simulated value which corresponds to the i^{th} observation;
$p_{p,}$	is the p^{th} prior estimate included in the regression;
$p_p'(p)$	is the p^{th} simulated value;
w_i	is the weight for the i^{th} observation;
w_p	is the weight for the p^{th} prior estimate.

The differences $[y_i - y_i^{'}(b)]$ and $[p_p - p_p^{'}(b)]$ are called residuals. Weighted residuals are calculated as $w_i^{1/2}[y_i - y_i^{'}(b)]$ and $w_p^{1/2}[p_p - p_p^{'}(b)]$. A more complete description

of regression with respect to UCODE_2005 is provided by Hill (1998), and (Hill and Tiedeman, in press for 2007).

During execution, UCODE_2005 substitutes parameters in model input files, runs the model, and extracts values from the output files to calculate simulated equivalents of the field observations. Each parameter is perturbed to calculate the sensitivities where the sensitivities and residuals are used to update the parameter values via the modified Gauss-Newton method. The solution is checked to determine if the problem has met the convergence criteria. Finally, after the optimization is completed, statistics are calculated for use in diagnosing inadequate data and identifying parameters that probably cannot be estimated given the current model and available data, evaluating estimated parameter values, and assessing how well the model represents the simulated processes. A flowchart representing the iterative process for UCODE is presented in Figure 3.4.

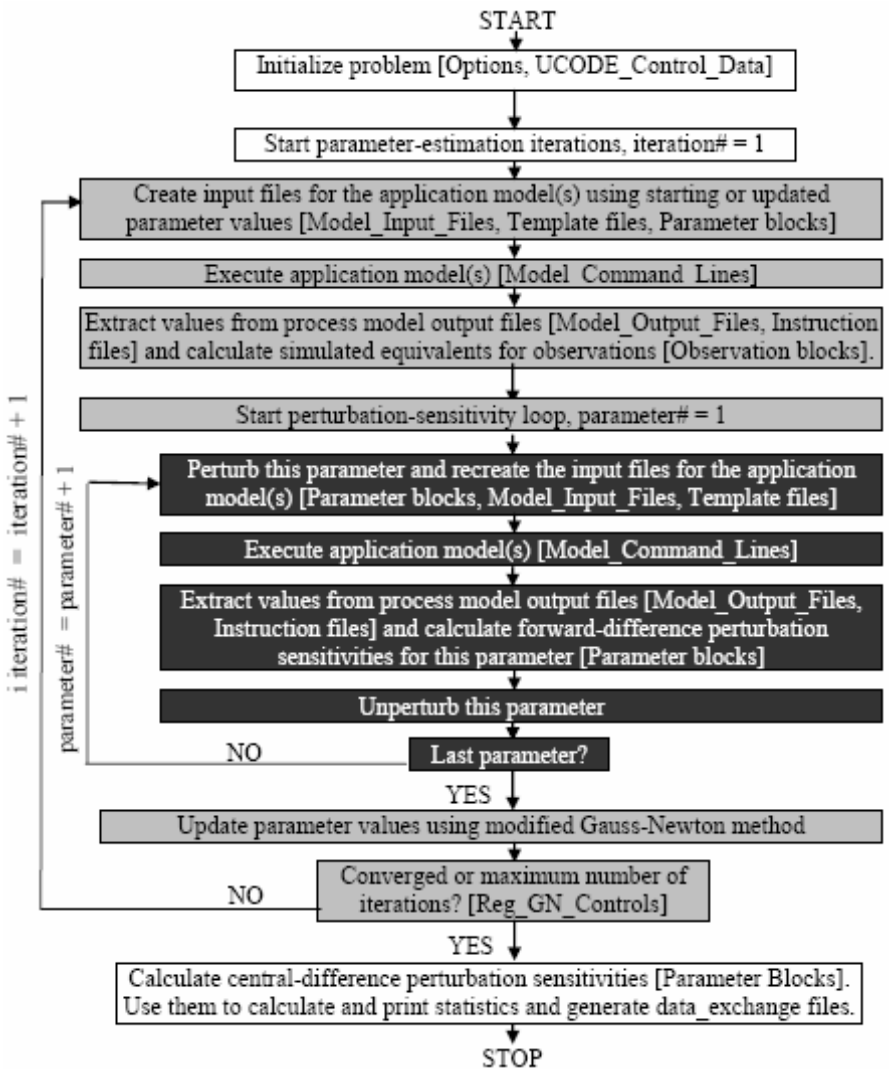

Figure 3.4: Flowchart describing major steps during the parameter estimation process in UCODE_2005, from Poeter et al., 2005.

Model Parameters

In order to improve the ground-water flow model calibration, the plume position in the north-south direction is included with head and stream flow observations. The following parameters are estimated: multiplication factors on the hydraulic conductivities of the basin for both layers; a multiplication factor on the ungaged mountain front recharge from the San Bernardino Mountains in the upper northeastern portion of the model domain; and the southeastern boundary conductance controlling flow into the basin (Figure 3.5 and Table 3.3). Also, an inflow of 10,000 ac-ft/yr (Danskin, personal communication, 2006) is diverted from the Zanja ditch to aid in the calibration process. All other parameters have the same values as in the Danskin model.

Alternative conceptual models of the source are considered for transport modeling. Parameters defining the source and dispersivity are estimated with regression (Table 3.3). Other transport parameters are assigned values as indicated in reports related to the basin (HSI, 1998; EIR, 2004). These values should be reconsidered in future work.

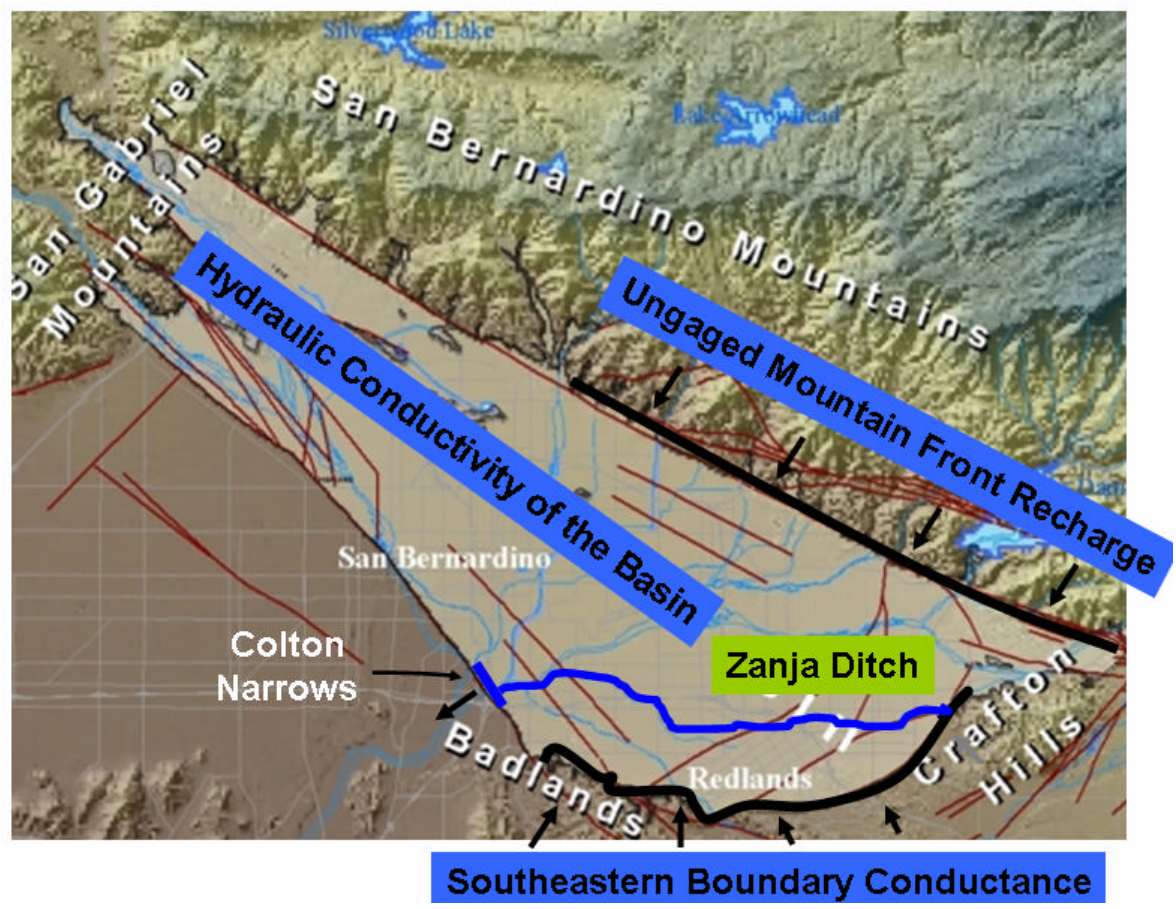

Figure 3.5: Location of boundaries for recalibration. Underlying image from Danskin, 2006.

Table 3.3: Parameters estimated by regression for the flow and transport models. Note Zanja is not an estimated parameter but is essential for explanation with respect to the modified model calibration process.

PARAMETER	DESCRIPTION	RATIONALE
HK Layer 1 Factor	Multiplication factor adjusting the hydraulic conductivity of layer one	Influences velocity in layer one
HK Layer 2 Factor	Multiplication factor adjusting the hydraulic conductivity of layer two	Influences velocity in layer two
Northeastern Ungaged Mountain Front Recharge Factor	Multiplication factor manipulating the value of recharge that is not gaged flowing onto the north-eastern surface of the basin	Influences both flow rates in response to adding stream flow to the Zanja ditch and the north-south position of the simulated plume
Zanja Stream Flow	Value of the stream flow rate entering the upper portion of the Zanja	Influences flow paths that control the north-south position of the simulated plume
Southeastern Boundary Conductance Factor	Conductance factor controlling flow through the southeastern boundary	Influences residuals on the southeastern boundary which are large and the north-south position of the simulated plume
Dispersivity	Longitudinal dispersivity	Value uncertain
Source Timing	Mass source timing	Influences east-west position of the plume
Mass	Mass of contamination introduced into the aquifer	Influences magnitude of concentrations
Mean Time of Mass Input	Mean of the statistical distribution	Influences the peak of the normal and lognormal statistical distributions used to represent mass input to the ground-water table
Variance	Variance of the statistical distribution	Influences the shape of the normal and lognormal distributions to represent mass input to the ground-water table

Observations for Parameter Estimation

Transient hydraulic heads, flows, and the north-south position of the TCE plume comprise the observation data for the flow model calibration. There are 15140 transient hydraulic head observations from 64 wells throughout the basin and 54 flow observations of differences in stream flow between gages from 1954 to 1998 as indicated in Table 1 of Danskin's 2006 report (Figure 3.6). There are 60 observations indicating the position of the plume is approximately 6 miles north of the southern border of the model domain and one observation indicating the final plume position at the end of the calibration period. Three-hundred six TCE concentration observations from 61 wells (Figure 3.6) over a twenty-four year period from 1980 to 2004 are used to calibrate the transport model.

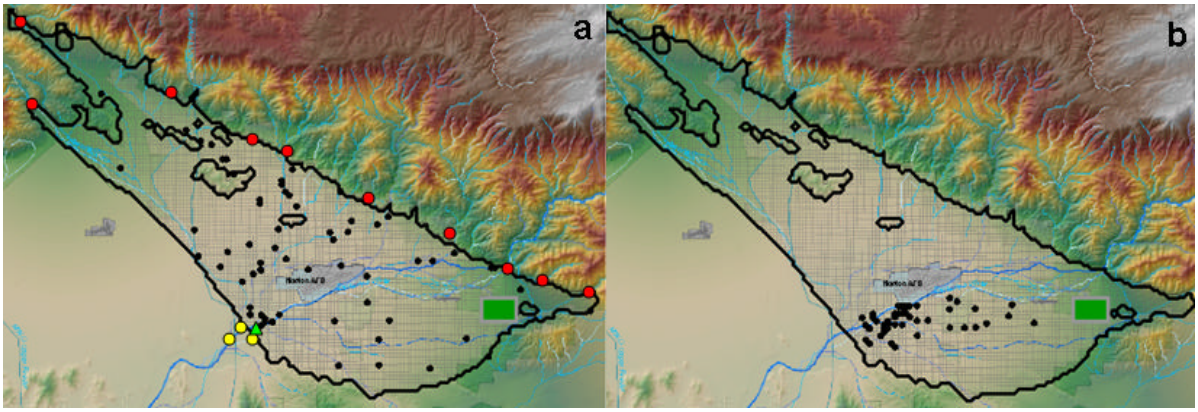

Figure 3.6: Observation locations for the flow model a) heads (black dots), inflow observations (red dots), outflow observations (yellow dots), final plume location (green triangle), and for the transport model b) wells (black dots) for concentrations.

UCODE_2005 requires observations to be weighted so that: "(1) the weighted residuals are all in the same units so they can be squared and summed in the least-squares objective function, and (2) to reflect the relative accuracy of the measurements." (Poeter, 2005). The weight on each observation is the inverse of the measurement variance. The weight makes the weighted squared residuals unit-less and assigns high weights to more accurate observations. Measurement variance is not provided in reports that list the observation data. Thus, assumptions are made for each type of observation. Initially, the following values are used to calculate variance for weighting: 1) hydraulic heads are assumed to be within +/-24.24 ft with 95% confidence, 2) stream flows and observed plume locations are assumed to be within +/-100% of measured values with a 95% confidence, and 3) 95% confidence intervals on concentrations are assumed to be +/-20% of the measured value for detected concentrations and +/-40% of the detection limit for censored values.

To confirm that the weighting is consistent with the model fit, the modeler strives for a (Calculated Error Variance) CEV with confidence intervals that include one. "If the fit achieved by the regression is consistent with the data accuracy as reflected in the weighting, the expected value of the CEV is 1.0." (Hill, 1998). The CEV is a statistic used to reveal how well the simulated values match the observations relative to their assigned weighting and is calculated as:

$$CEV = \frac{S(b)}{ND - NP} \qquad (3.3)$$

where:
ND is the number of observations;
NP is the number of parameters;
S(b) see Equation 3.2.

Values of the CEV far from unity indicate that the model fit is inconsistent with the weighting. Poeter and Hill (1997) summarize: "Values below one signify that the model fits the observations better than was indicated by the assigned weighting and values greater than one reflect that the model fit is not as good as indicated by the assigned weighting, which is due to expected measurement and model error typically represented in weighting." Significant deviations from unity are indicated if 1.0 falls outside the lower and upper 95% confidence intervals of the CEV.

The initial weights produced a CEV of 65.9 with intervals ranging from 64.5 to 67.5. These are adjusted (Table 3.4) to obtain a CEV closer to unity, thus the final weights are consistent with the quality of fit of the model.

Table 3.4: Summary of observations and weighting scheme. Note: SD is standard deviation and CV is coefficient of variation. Final values of the concentrations represent detected and censored observations, where the * applies to censored observations.

Observation Type	Number of Observations	Weighting Scheme	Final Value
Hydraulic Heads (ft)	15140	SD	98.43
Stream Flows (cfs)	54	CV	15252./(observed value)
Plume Locations (ft)	61	CV	0.5
Concentrations (ppb)	306	SD	32.67*, 16.33

Summary statistics with respect to concentration observations (Table 3.5) shows the percentages of observations that are either above or below detection limit. Also the mean, median, and the maximum concentration are shown.

Table 3.5: Summary statistics for the TCE concentration observations. All values in ppb.

% Detect	% Censored	Mean	25th percentile	Median	75th percentile	Maximum Concentration
86	14	23.0	1.4	10.1	30.4	163.1

Comparison of Calibration Quality for the Danskin and Modified Models

The only differences between Danskin's and the modified model are that 10,000 ac-ft/yr of flow is diverted from Mill Creek to the head of the Zanja ditch because this diversion is not included in Danskin's model, but it occurs in the field. Ten-thousand acre feet per year is used because it is the maximum flow that Danskin felt representative of the field conditions, (Danskin, personal communication, 2006). The other difference is values of the parameters (Table 3.3) are adjusted to obtain a better fit to the observed values. Each model is evaluated using the following criteria: 1) convergence to a reasonable tolerance where the change of parameter values is less than 1% between parameter estimation iterations; 2) realistic optimized parameter values; 3) non-correlated optimized parameters; 4) acceptable model fit; and 5) randomly distributed residuals with respect to time, space, and simulated values.

Calibration results of the modified model show an optimal fit to the data is obtained with 1) the northeastern mountain front recharge approximately 5% of Danskin's value, albeit with insensitivity causing removal of the parameter during the course of the regression; 2) the hydraulic conductivity multiplier of layers one and two a factor of 2.166 and 0.693 of Danskin's values, respectively, with insensitivity causing removal of the layer-one multiplier; and 3) the conductance of the southeastern boundary increased by a factor of 5.0, also with insensitivity removing this parameter during the course of the regression. Final parameter values are listed in Table 3.6. The Sum of Squared

Weighted Residuals (SOSWR) of the modified model is approximately one-half that of the Danskin model. The CEV is below one for both models indicating that the model fit is better than anticipated given the weights assigned to the observations. The lower CEV for the modified model reflects the improved fit for the same observation weights. Statistics including the SOSWR, CEV, and the upper and lower 95% confidence intervals of the CEV are shown in Table 3.7.

Table 3.6: Ratio of optimized parameter values for the modified flow model to those of Danskin's model.

	Hydraulic K Factor Layer One	Hydraulic K Factor Layer Two	Northeastern Mountain Front Recharge Factor	Southern Boundary Conductance Factor
Modified Model	2.166	0.6933	0.0454	5.0

Table 3.7: Comparison of the SOSWR and the CEV for the Danskin and modified flow models.

	SOSWR	CEV Lower 95% Interval	CEV	CEV Upper 95% Interval
Danskin Model	12217	0.78	0.80	0.82
Modified Model	6563	0.51	0.52	0.53

Graphical measures of model error and the quality of calibration can be evaluated using several graphs. For example, weighted residuals versus simulated equivalents may identify model bias. An unbiased model has a uniform distribution of the residuals around zero with roughly equal number of positive and negative residuals, thus the graph

should have a slope and y-intercept of zero, with an R^2 near zero. The differences between models are subtle, but indicate a slightly better calibration for the modified model in that the modified model is closer to zero than the Danskin model for all of those measures (Figure 3.7). A graph of weighted observed values versus weighted simulated equivalents also evaluates model bias. For an unbiased model, this graph would have a slope of one and y intercept of zero, with an R^2 near one. In this case the graphs show similar trends, however, the modified model has a more desirable intercept and R^2 (Figure 3.8).

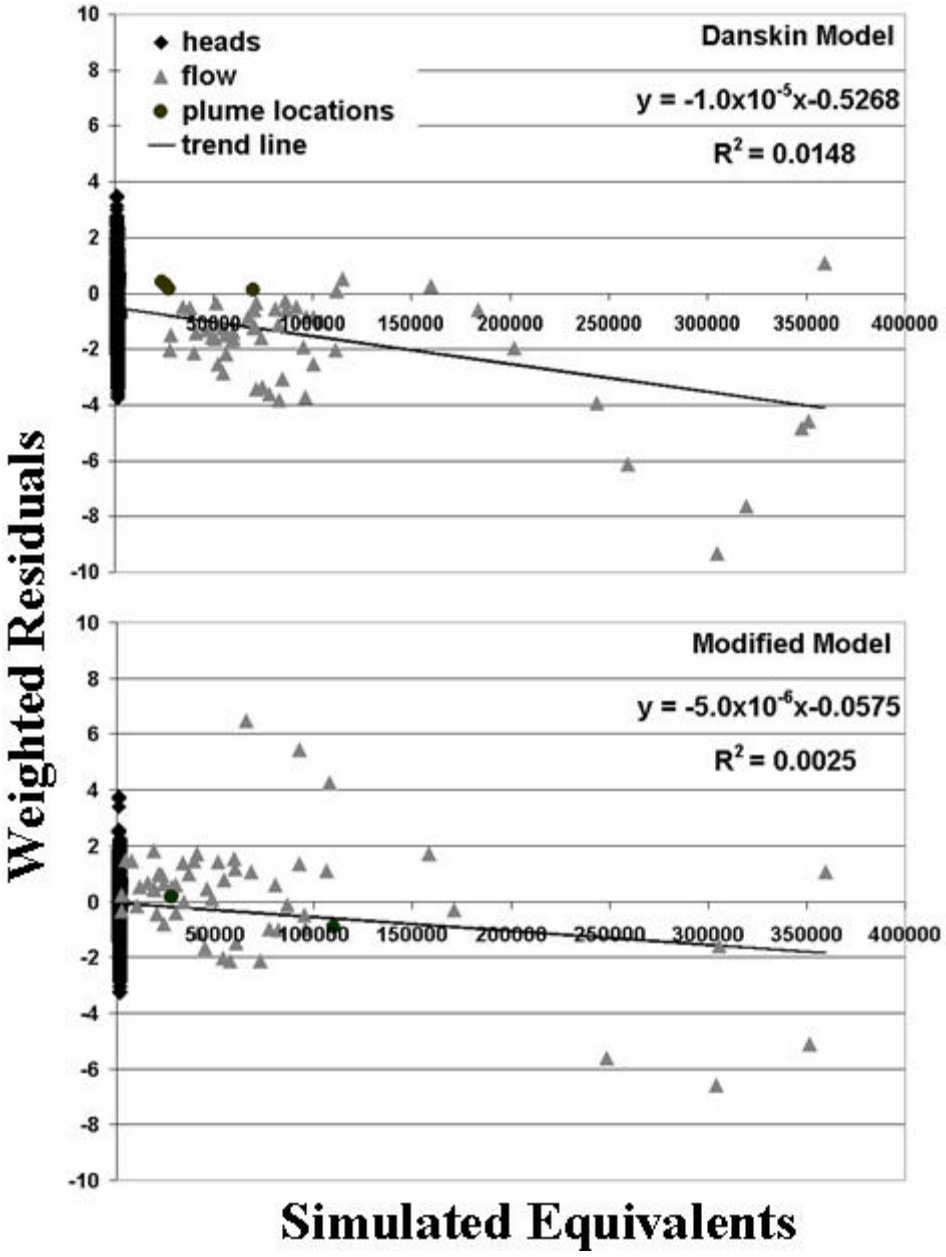

Figure 3.7: Weighted residuals versus simulated equivalents for the Danskin and modified flow model.

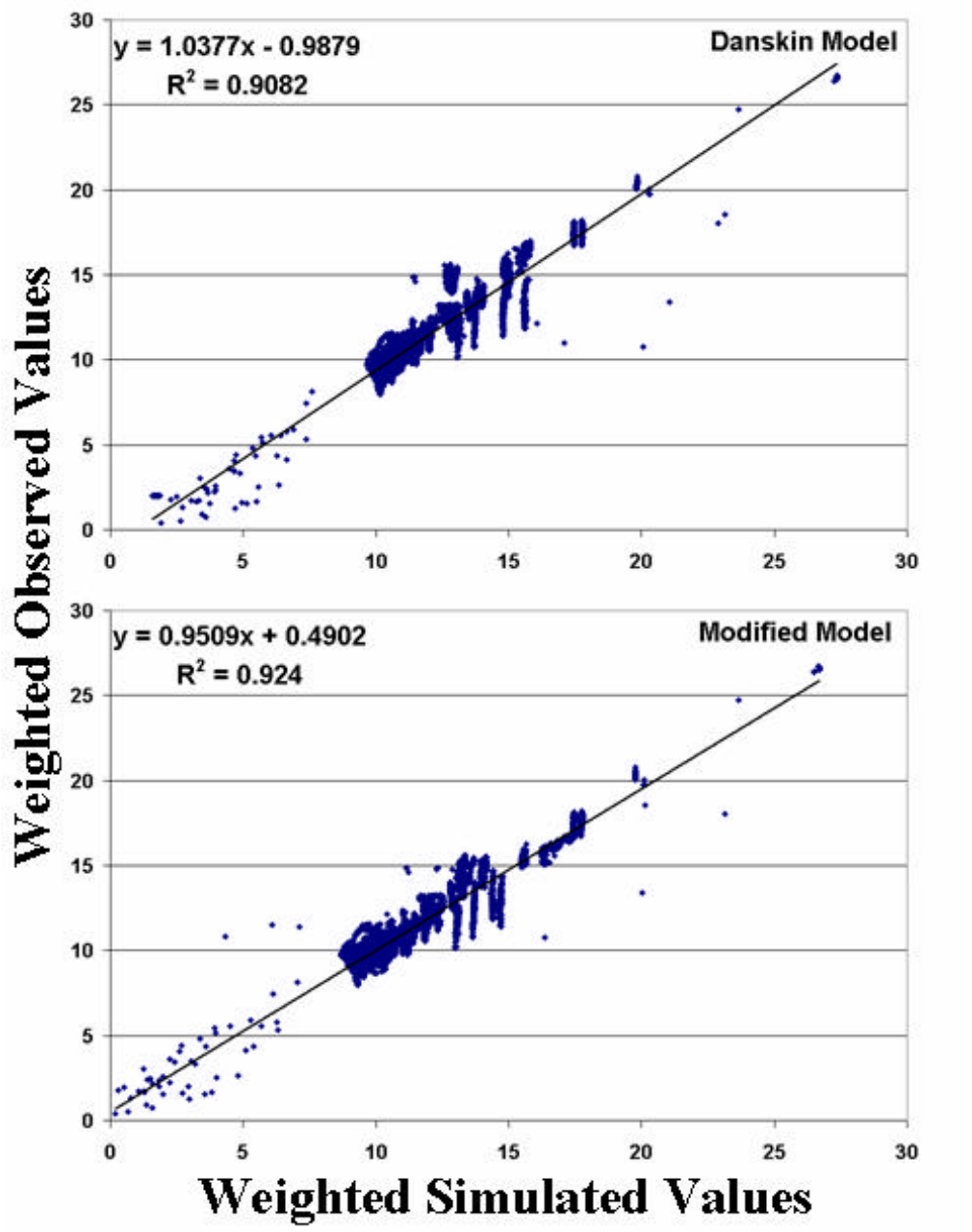

Figure 3.8: Weighted observed values versus weighted simulated values for the Danskin and modified flow model.

Weighted residuals versus standard normal statistics should form a straight line on a normal probability graph. If the weighted residuals form a straight line on the normal probability graph, it is likely that they are independent and normally distributed. The graphs of both the Danskin and modified models exhibit nonlinearity (Figure 3.9). Deviation from linearity indicates a greater probability that the weighted residuals cannot be considered as random and normally distributed. Hence, this requires the weighted-residual test to be conducted which entails generating and plotting randomly generated independent normally distributed and correlated normally distributed numbers to evaluate the source of the deviation. If similar deviations are apparent for the independent values then the nonlinear shape of the weighted residuals could be the result of too few observations for computing residuals. If similar deviations between the weighted residuals and the independent normally distributed numbers are not apparent, then the trend between weighted residuals and correlated normally distributed numbers should be considered. If the weighted residuals show trends similar to the correlated deviates, then the nonlinear shape is likely a result of regression-induced correlation. However, if the graph exhibits dissimilar deviations then the nonlinearity is likely a result of an incorrect conceptual model or bias in the observation data. The weighted residual tests for the Danskin model suggests that the conceptual model may be incorrect or the data may be biased since both independent and correlated normally distributed numbers exhibit dissimilar deviations from the weighted residuals. With respect to the modified model, the trend of the weighted residuals is more similar to the random independent and

correlated deviates, particularly in the central portion of the distribution, suggesting the conceptual model has been improved although there may be room for further improvement (Figure 3.9).

Mapping weighted and un-weighted residuals in space and graphing them in time provides insight into spatial and temporal bias. If there is no spatial bias, the map of residuals will exhibit a random pattern of positive and negative values, as well as large and small residuals. Positive residuals are more uniformly spread throughout the basin in the modified model as compared with the Danskin model (Figure 3.10). The residuals through time should exhibit a narrow horizontal band centered about zero. The modified model exhibits a trend with a slope and intercept slightly closer to zero, albeit with a slightly smaller R^2 value, indicating less temporal bias than the Danskin model (Figure 3.11).

In conjunction with the residual analysis graphs, the observed values of basin inflow minus outflow are compared with the simulated inflow minus outflow values for both the Danskin and modified models. Finally, the location of the simulated plume (using initial estimates of transport parameters and source character) is also examined. The modified model provides a better fit to the difference in flow observations (Figure 3.12). Moreover, the location of the plume simulated by the modified model is closer to the observed location of the plume in the field (Figure 3.13).

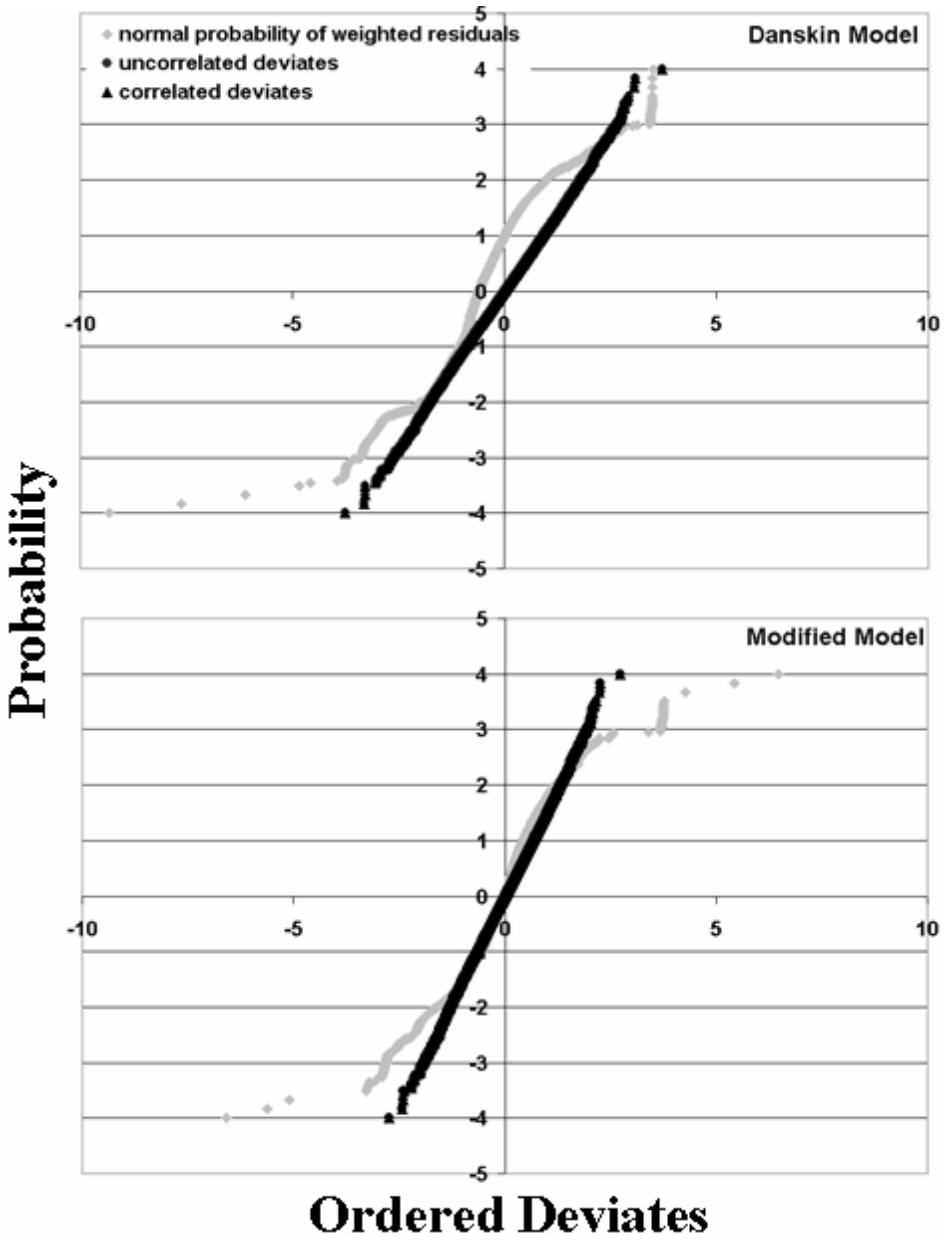

Figure 3.9: Normal probability graph showing trend of weighted residuals, uncorrelated and correlated deviates for the Danskin and modified flow model.

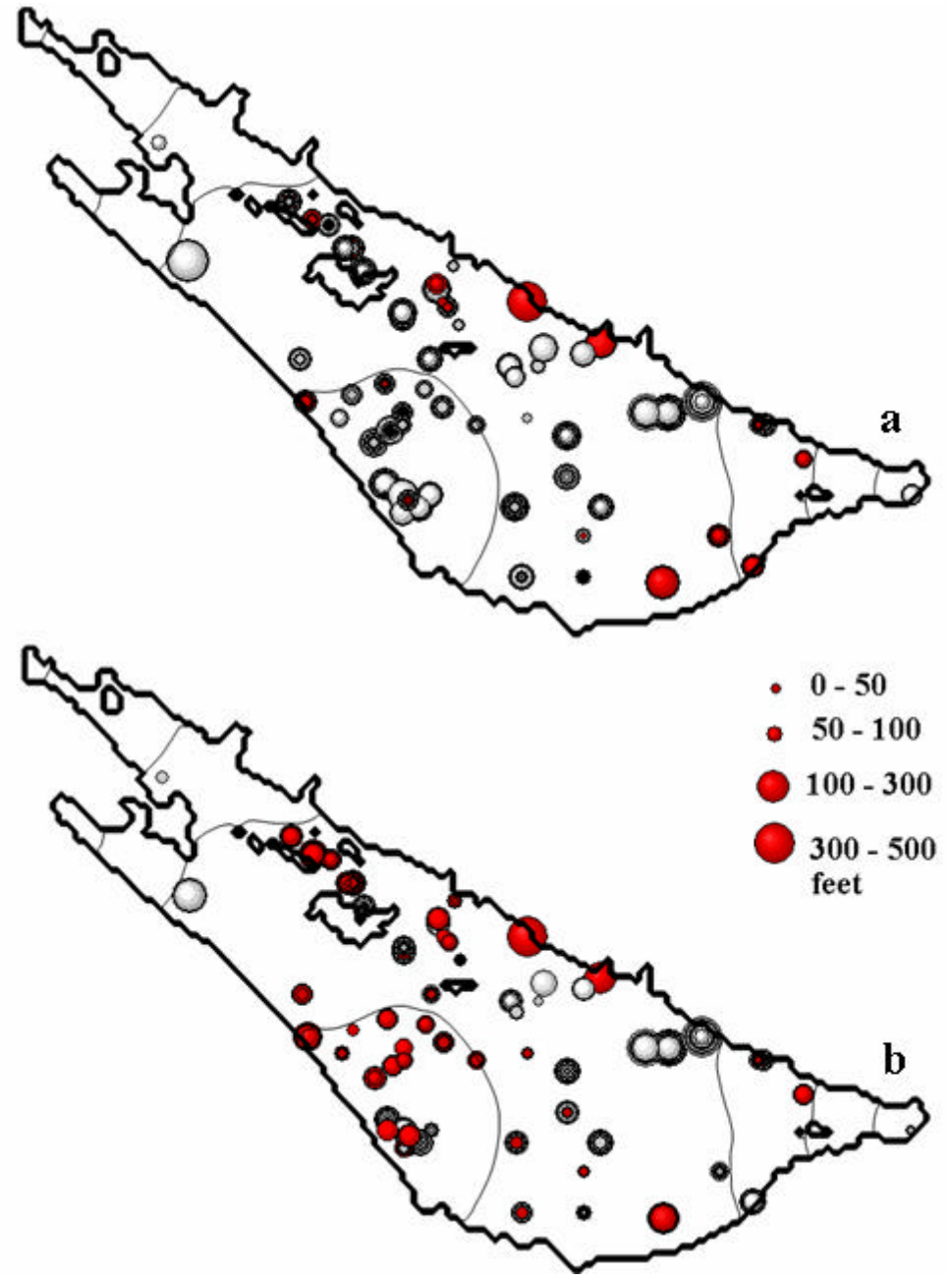

Figure 3.10: Spatial distribution of residuals for all times, a) Danskin model, b) modified model. Red circles represent positive residuals and white negative.

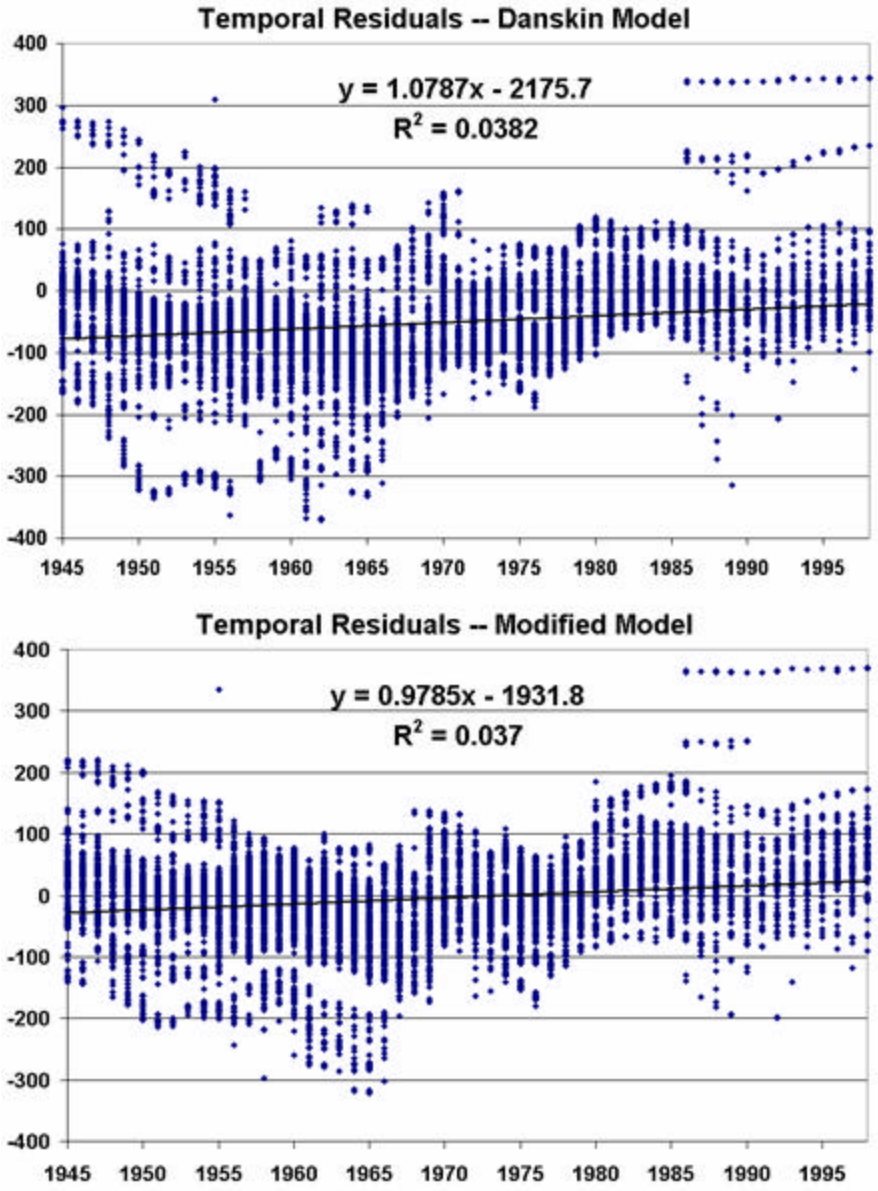

Figure 3.11: Temporal residuals for the Danskin and modified flow models.

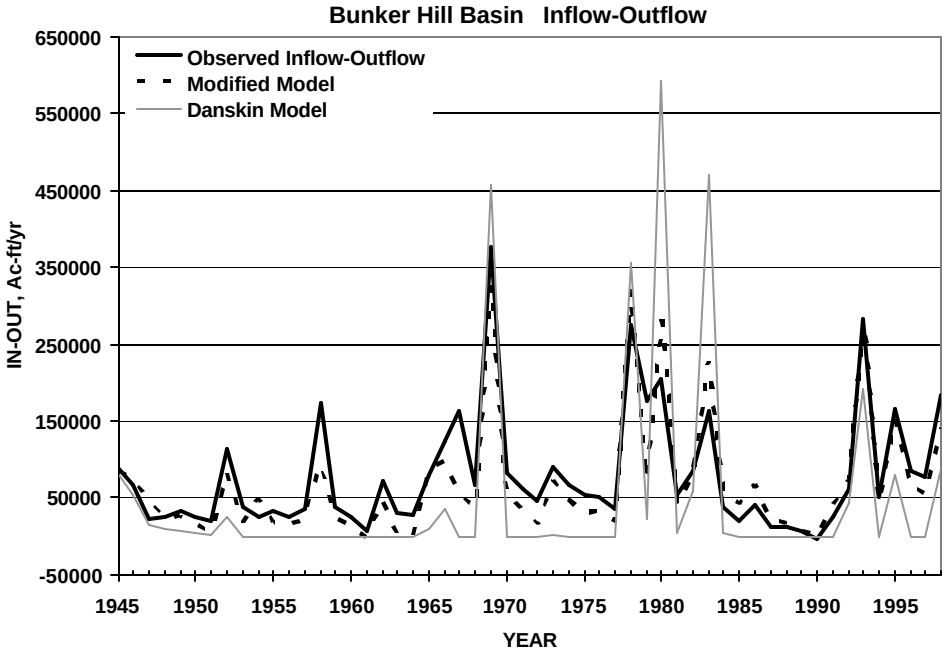

Figure 3.12: Observed surface water inflow minus outflow for field observations compared to the Danskin and modified flow models.

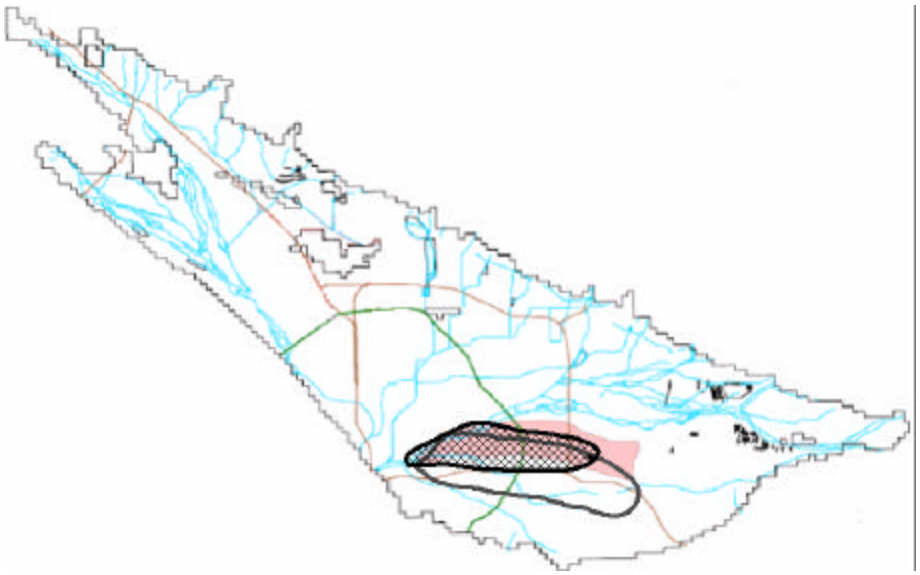

Figure 3.13: Comparison of the spatial locations of the simulated TCE plume after flow calibration. The unfilled outline is the 5ppb contour using Danskin's flow model and initial estimates of transport parameters. The cross-hatched plume is the 5ppb contour simulated using the modified flow model. The pink shaded area is the 5ppb contour of measured concentrations from EIR, 2004.

Verifying Unique Optimal Parameter Values

The combinations of parameter values that yield the lowest SOSWR are considered the optimal parameter values. To confirm uniqueness of the optimized values (Table 3.5) it is good practice to repeat parameter estimation with different starting parameter values confirming that similar optimized values are obtained. This is accomplished by starting regressions at either the upper or lower confidence intervals reported by UCODE_2005, or different parameter combinations of the values at those limits. If the resultant values are within one standard deviation of the prior estimates, it can be assumed that the optimal values are unique.

For this project, parameter uniqueness is evaluated using three regression runs with different starting parameter values. The results of the regressions reveal the final parameters are close estimates of each other, but various parameter values showed insensitivity during regression and hence, were removed from the estimated set. The starting parameter values for each regression, final estimated values, and the SOSWR with respect to each set of optimal parameters are listed in Table 3.8. Non-uniqueness occurred for both the multiplication factors on the hydraulic conductivity of layers one and two (Figure 3.14). However, the northeastern mountain front recharge factor and the southeastern boundary conductance factor both are unique (Figure 3.15). Results of the uniqueness test depict the final optimal parameter values for each run with the upper and lower 95% linear confidence interval. To define the solution as unique, we expect the

estimated values to fall within half of a 95% confidence range of the parameter set with the lowest SOSWR. It is important to note that the illustrated intervals are calculated assuming linearity.

Nonlinear intervals may reveal that the solution is more unique than concluded by this evaluation. The large confidence intervals on the mountain front recharge and the boundary conductance are due to small sensitivities to the observation data which can be improved by collecting more data or reposing the problem. Regardless, the final estimates are similar for each regression, so it is suggested that nonlinear confidence intervals be calculated in the future, and uniqueness be re-evaluated, but this is beyond the scope of this work.

The improved fit and more desirable distribution of residuals in the modified model with the lowest value of SOSWR indicates that it is more representative of the ground-water flow system in Bunker Hill Basin than the original Danskin model. Hence, the modified model is used for evaluation of the source function in the remainder of this report.

Table 3.8: Initial and final parameter values for three regressions. Note that shaded cells indicate the final estimated value before the parameter was omitted from the regression due to insensitivity.

Parameters	Initial Values Run 1	Final	Initial Values Run 2	Final	Initial Values Run 3	Final
K Factor Layer One	2.17	**2.16**	2.50	**2.51**	3.0	**2.3**
K Factor Layer Two	0.68	**0.69**	1.00	**1.00**	0.10	**0.51**
Mountain Front Recharge Factor	0.091	**0.045**	1.50	**1.51**	0.50	**0.59**
Boundary Conductance Factor	5.0	**5.0**	10.0	**10.0**	10.0	**10.0**
SOSWR		**6563**		**9367**		**10122**

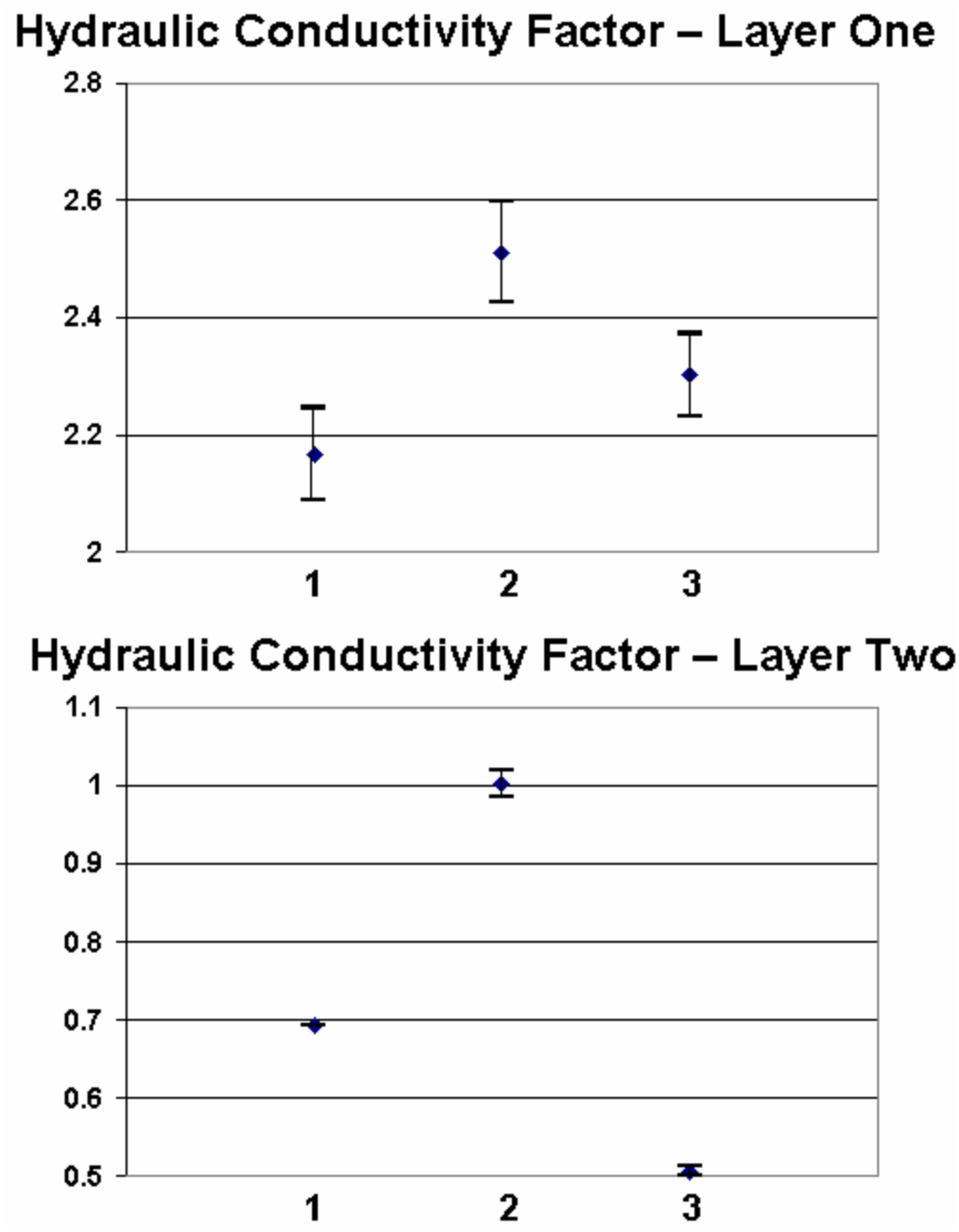

Figure 3.14: Optimal parameter values and their upper and lower 95% confidence intervals for three regression runs. Diamonds are the optimal values and error bars represent the upper and lower linear 95% confidence intervals. Ideally all points should fall within the adjacent point's error bars.

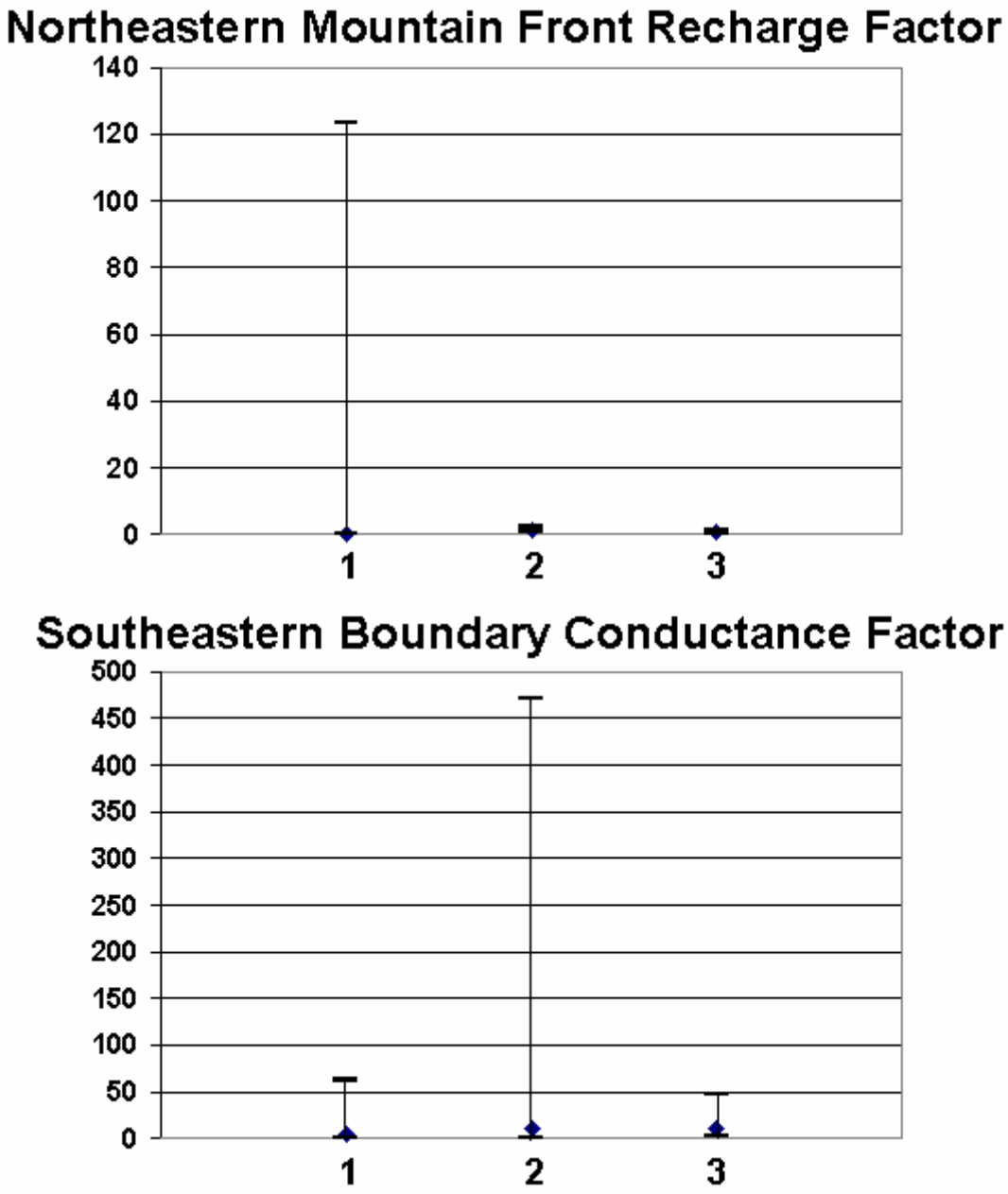

Figure 3.15: Optimal parameter values and their upper and lower 95% confidence intervals for three regression runs. Diamonds are the optimal values and error bars represent the upper and lower linear 95% confidence intervals. Ideally all points should fall within the adjacent point's error bars.

CHAPTER 4: USE OF OBSERVATIONS BELOW DETECTION LIMIT FOR MODEL CALIBRATION

Censored data is traditionally assessed using four substitution methods such that the values are replaced with: 1) the value of the detection limit; 2) one-half the detection limit; 3) zero; or 4) nothing in that they are not used in the regression. Assuming that we analyze nondetect data in a manner reflecting we know only that the value is below the detection limit, i.e., the censored-residual approach, a more realistic representation of the system should be realized. This chapter explores three cases to evaluate the censored-residual approach and compares the results with the four alternative approaches. The three cases are: 1) a synthetic homogeneous source and aquifer; 2) a synthetic heterogeneous source and aquifer; and 3) a site where TCE is migrating in the Bunker Hill Ground-Water Basin.

Synthetic Cases

The first synthetic case is a homogeneous aquifer with a constant mass input to the aquifer for a period of 10 days. The second case is a heterogeneous aquifer with variable mass input to the aquifer spanning a period of 10 days. Both synthetic cases assume the contamination is uniformly distributed vertically throughout a 9 meter thick aquifer represented by a finite-difference, block-centered grid using MODFLOW-2000 (Harbaugh et al., 2000). The grid domain is 100 columns in the x-direction and 50 rows

in the y-direction with uniform cell dimensions of 3 by 3 meters comprising a model domain of 300 meters by 150 meters (Figure 4.1). The boundary conditions include no-flow boundaries on the north and south sides of the model grid and constant head boundaries on the east and west producing a ground-water flow gradient of 1.0 meter/meter from west to east. The potential for a line-source of recharge is included in the conceptual model and recharge is applied at the start of the regression, but the 'true' rate of recharge is zero in the synthetic models.

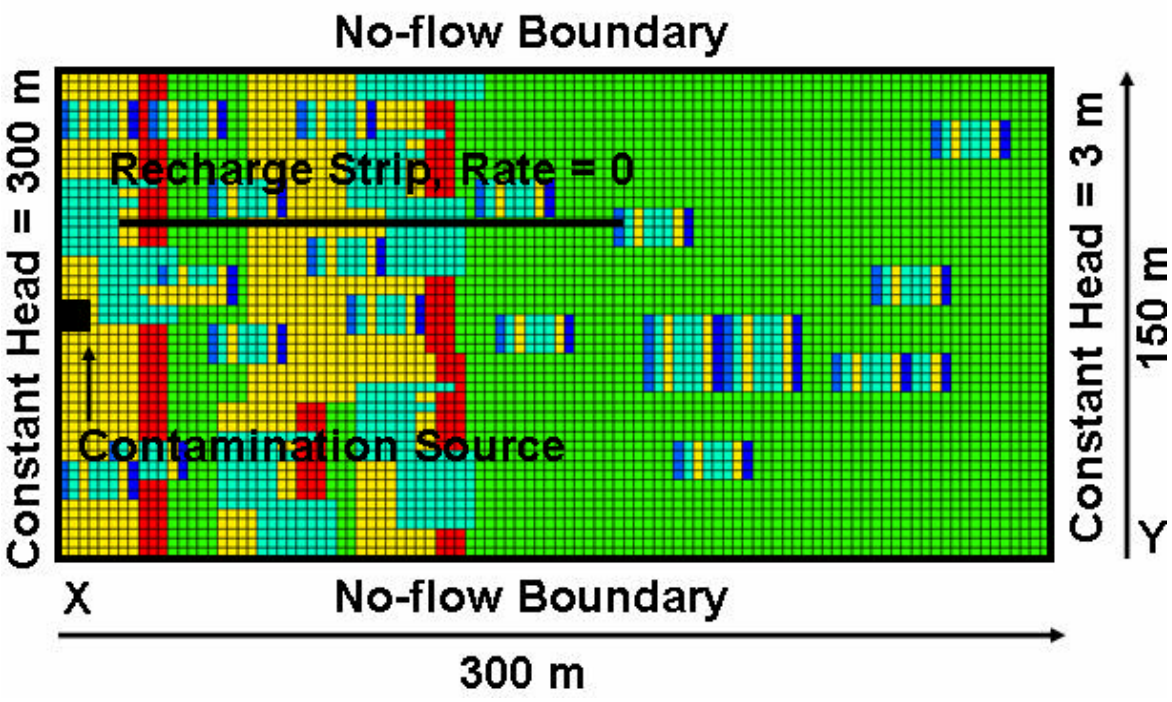

Figure 4.1: Model grid and boundaries for the synthetic cases showing the hydraulic conductivity distribution for the heterogeneous case. Individual hydraulic conductivity values in ft/day such that red represents 25, yellow 20, green 15, aqua 10, light blue 5, and dark blue 3.

Transport modeling is accomplished using MT3DMS (Zheng and Wang, 2005) with the same boundaries and spatial discretization as the flow model. Retardation is zero, longitudinal dispersivity is 3 meters, and transverse dispersivity is 0.15 meter. Observation locations are delineated throughout the aquifer as indicated by dots in Figure 4.2. Observations are taken from the "true" synthetic model with a detection limit defined as 5 mg/L. Concentrations (after ten days of transport) simulated using "true" model parameter values and plumes generated using the parameter values defined at the start of the regression are shown for both the homogeneous and heterogeneous cases (Figure 4.2). The estimated parameters include longitudinal dispersivity, recharge along the line source, and porosity.

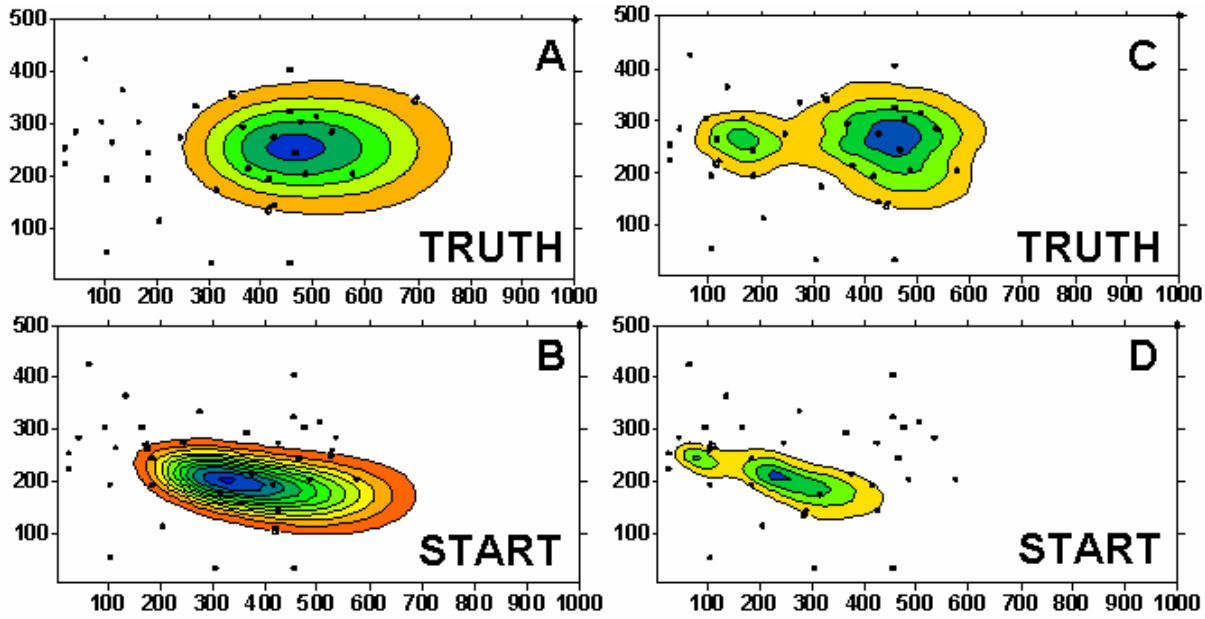

Figure 4.2: Concentrations after 10 days of transport as simulated using the true parameter values and the values at the start of the regression. A) true plume configuration in homogeneous aquifer; B) starting plume in homogeneous aquifer; C) true plume in heterogeneous aquifer; D) starting plume in heterogeneous aquifer.

Synthetic Case Results

In general, the censored-residual approach produces better calibration statistics and more accurate parameter values than substitution methods. Calculated residuals are much smaller when the censored-residual approach is used. For instance, the regression quality plot depicting weighted residuals versus simulated values forms a narrower band around zero as compared with the approach where the detection limit is used for censored observations (Figure 4.3). Similar results are found for the other alternative methods, but these are not shown.

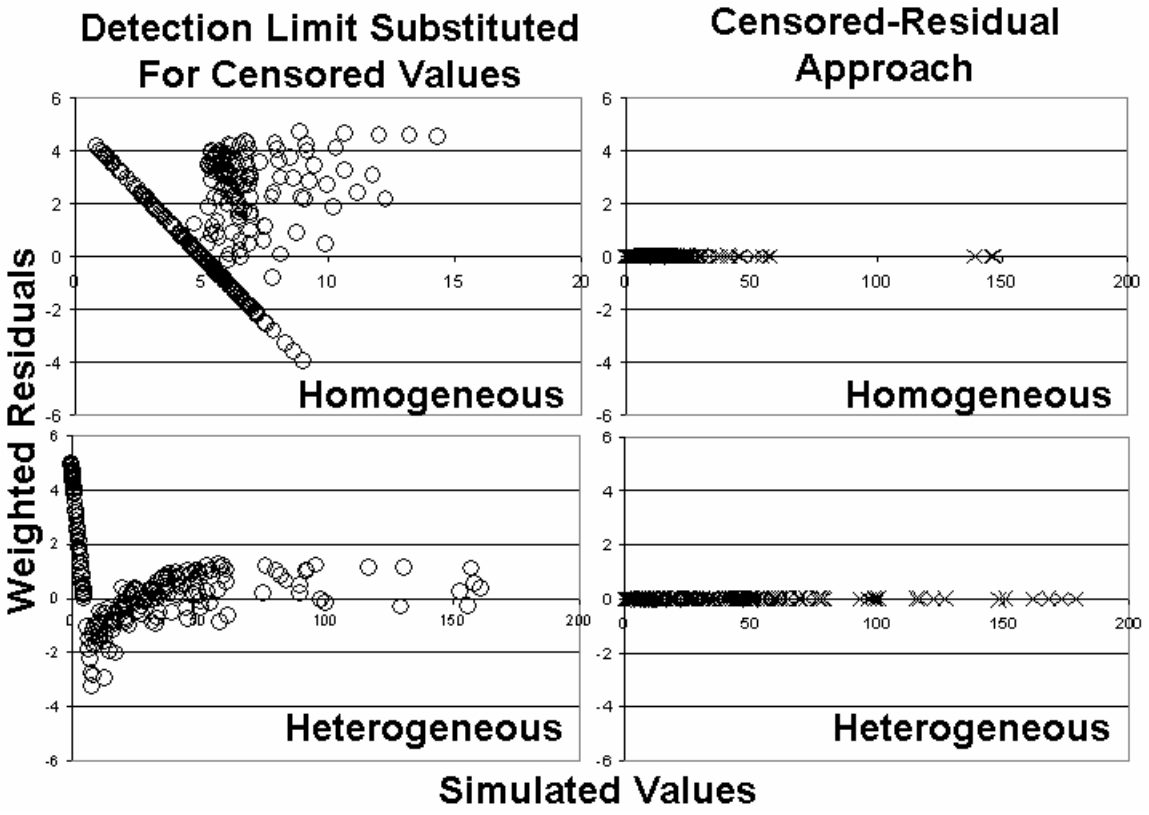

Figure 4.3: Weighted residuals versus simulated values for the synthetic cases with respect to treatment of censored values.

Parameter estimation converges for all the homogeneous cases. The censored-residual approach produces the best statistics and most accurate parameters, followed by the case for which censored values are completely omitted from the regression. Substitution of zero for the censored values delivers smaller values of longitudinal dispersivity and concentration than the true values, as would be expected if the observed plume is confined to the zone where detections are noted. Unreasonably large longitudinal dispersivities are estimated when one-half the detection limit is substituted for the observation, or the detection limit is substituted for the observation, as would be expected if higher concentrations are observed at the location of the censored values.

Parameter estimation also converged for each heterogeneous simulation. Again, the best results are obtained when invoking the censored-residual approach. The next best results are obtained by removing censored values from the regression. Use of zero for the censored data again results in estimation of smaller longitudinal dispersivity and concentration values than the true values in the synthetic model, and large longitudinal dispersivities are estimated when the censored values are assigned one-half the detection limit, or the detection limit. The final parameter values, Standard Error of the Regression (SEOR), SOSWR, and the true parameter values of the synthetic case are listed (Table 4.1).

Table 4.1: Final optimized parameter values and calibration statistics for the synthetic cases.

CASE	Longitudinal Dispersivity	Porosity	C1	C2	Recharge	SOSWR	SEOR
Homogeneous – TRUE	**10**	**0.3**	**500**		**0**		
censored-residual approach	10	0.300	502		9.1×10^{-7}	85.8	0.48
censored values removed	10	0.300	503		1.7×10^{-5}	130.2	0.83
censored values at zero	7.7	0.302	468		6.4×10^{-5}	333.0	0.95
censored values at detection limit	2142	0.310	1345		2.3×10^{-5}	1733.0	2.1
censored values 1/2 the detection limit	2229	0.304	610		3.9×10^{-5}	2522.9	2.6
Heterogeneous – TRUE	**10**	**0.3**	**2000**	**500**	**0**		
censored-residual approach	10	0.300	2008	504	1.5×10^{-4}	81.5	0.47
censored values removed	10	0.300	2008	504	1.6×10^{-4}	81.5	0.70
censored values at zero	7.6	0.301	1851	449	1.6×10^{-4}	351.1	1.0
censored values at detection limit	32	0.323	2126	512	1.4×10^{-4}	3563.8	3.1
censored values 1/2 the detection limit	12	0.305	1769	417	1.5×10^{-4}	3816.1	3.2

Results show the superiority of some substitution methods relative to others, but all are inferior to removing the censored values, or using the censored-residual approach. Removing the censored data provides accurate estimates for these cases because the remaining data fully capture the character of the plume. When the substitution methods are invoked, the regression uses concentrations equal to the substituted values, giving the same value of concentration to all censored data. This is not a realistic assumption. The zero substitution method is better than the one-half or detection limit substitution for these cases because the concentrations at the censored locations are closer to zero than to the other substituted values.

Given that the results are so similar, one might ask why it is concluded the censored-residual approach is best? The censored-residual approach is most advantageous because it allows all the data to be included, and in some cases including all the available data will better define the plume. Figure 4.4 delineates a situation where that is the case, and is a situation to be tested in future experiments.

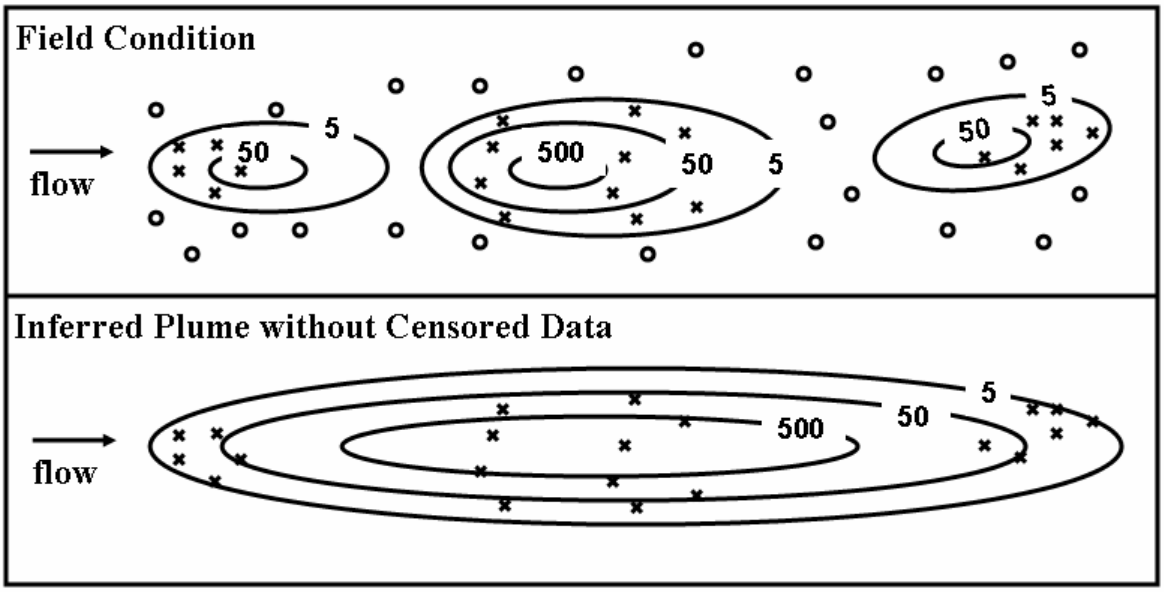

Figure 4.4: One scenario in which including censored-data rather then removing data distinguishes the field situation. X's represent detect data and O's represent censored data.

The plumes simulated by the calibrated models after ten days of transport closely resemble the true plume for the synthetic tests, except for the homogeneous and heterogeneous cases when the censored values are at their detection limit, and for the homogeneous case when the censored values are replaced by one-half the detection limit. The best SOSWR and residual graphs are obtained for the censored-residual approach followed by the approach in which censored values are completely removed from the regression. Use of zero for censored data is better than substituting the detection limit and the least impressive results are generated by substituting one-half the detection limit. The relative ranking of alternative substitution approaches depends on the character of

the actual values, whereas the censored-residual approach does not purport any knowledge about censored values beyond the fact that they are below detection limit.

The simulated plumes after ten days of transport (using the estimated parameter values) for the synthetic cases are depicted in Figure 4.5. In the homogeneous case when the detection limit or one-half the detection limit are substituted for censored values, the SOSWR surface is flat (the solution is non-unique) so the estimates are not reliable. However, as is expected if the plume is widespread (i.e., if these values were large as indicated by substituting values above the true values), the dispersivity estimate is large, which leads to the same value of concentration throughout the model domain, thus no contours are depicted for Figures 4.5D and 4.5E.

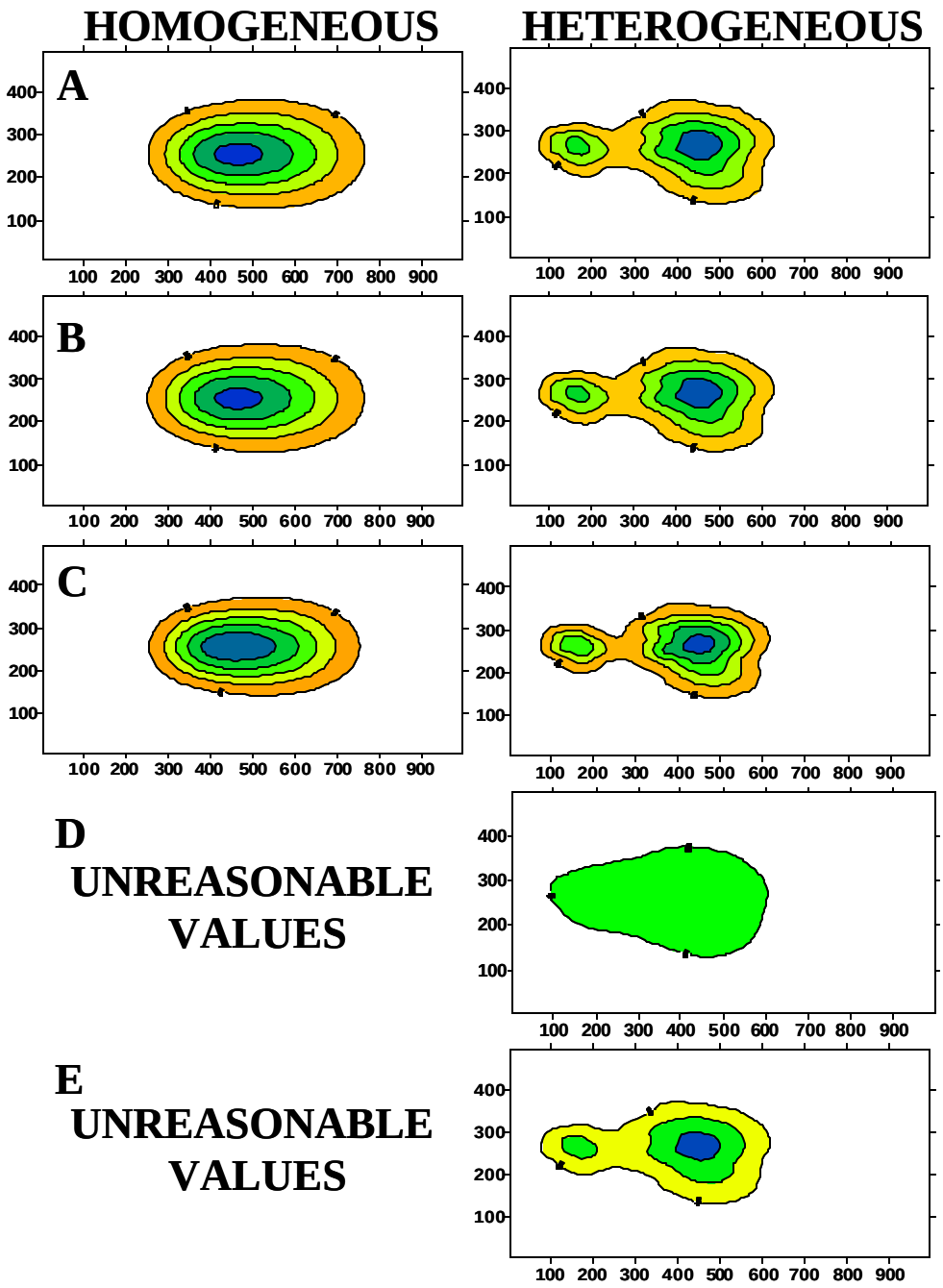

Figure 4.5: Calibrated plumes after 10 days of transport all contoured at 5 mg/L intervals. A) censored-residual approach; B) censored values removed; C) censored values replaced with 0; D) censored values replaced with detection limit, E) censored values replaced with one-half the detection limit.

Field Application

The censored-residual approach is used to estimate the character of the source for the TCE plume in the Bunker Hill Basin. All parameters mentioned in the results of Table 4.2 will be discussed in Chapter 5. This example is included in this Chapter to provide a field example using the censored-residual approach.

Results of Field Application

The calibrated model of TCE migration in Bunker Hill Basin has smaller SOSWR and SEOR values when the censored-residual approach is used as compared with the substitution methods. However, the substitution approaches do not attain the same relative rank of calibration statistics as found for the synthetic cases (Table 4.2). That is, assigning zero to the censored values ranks higher than removing the censored values. As mentioned in the assessment of the synthetic cases, the relative ranking of alternative substitution approaches depends on the character of the actual values, whereas the censored-residual approach does not purport any knowledge about censored values beyond the fact that they are below detection limit. Given that the synthetic problem yields more representative parameter values when the censored-residual approach is invoked, we conclude the estimated optimal parameter values using the censored-residual approach are more representative than those obtained using the other substitution methods.

Table 4.2: Final parameter values for the field application with respect to treatment of censored values.

	Longitudinal Dispersivity (ft)	Source Timing (year)	Mass (lbs)	Mean Time of Release (year)	Variance of Timing ($year^2$)	SOSWR	Upper 95%	SEOR	Lower 95%
censored-residual	327	28	19090	13	60	167	0.77	0.78	0.92
replaced with 0	419	21	25840	29	60	170	0.77	0.79	0.92
values removed	419	21	25840	29	60	170	0.79	0.86	0.94
replaced with 0.5	509	22	25280	30	58	181	0.80	0.82	0.95
at detection limit	512	22	25670	30	57	181	0.80	0.82	0.95

CHAPTER 5: ESTIMATING CONTAMINANT SOURCE HISTORY USING NONLINEAR REGRESSION AND AVERAGING OF ALTERNATIVE CONCEPTUAL MODELS

Models cannot entirely represent all the subtleties of ground-water systems, as they are only mere approximations of nature. For instance, reasonable alternative models of a system can yield similar calibrations and yet provide substantially different results (Hojberg and Refsgaard, 2005). To explore this, we use various conceptual models to estimate source history and examine alternative source functions using both nonlinear regression and model averaging.

Alternative Conceptual Models

Three important attributes distinguish sources of ground-water contamination: (1) their degree of localization, (2) their loading history, and (3) the type of contamination entering the system (Domenico and Schwartz, 1990). The available concentration data make it impossible to estimate a unique mass for each year, so we evaluate functions that will distribute the mass in time using only a few parameters. We consider four alternative source functions to represent TCE loading history, which are: an initial estimate of the possible mass distribution proposed by a stakeholder, a uniform distribution represented by a step function, a normalized truncated normal distribution and a normalized truncated lognormal function. For each conceptual model a set of

parameters is estimated to obtain a simulation that best matches the observed concentration data (Table 5.1, Table 3.3). Computer programs that print mass as a function of time using the estimated parameter values for each source conceptualization are described in the appendix and included on the CD distributed with this report.

Table 5.1: Parameters of interest for alternative conceptual models. The word underlined in this table is used to identify the parameter in the discussion.

Stake Holder	Step Function	Modified Truncated Normal Function	Modified Truncated Lognormal Function
Longitudinal Dispersivity	**Longitudinal Dispersivity**	**Longitudinal Dispersivity**	**Longitudinal Dispersivity**
Source Timing Start of source in years after 1945	**Source Timing** Start of source in years after 1945	**Source Timing** Start of source in years after 1945	**Source Timing** Start of source in years after 1945
Total Mass for Entire Period	**M1** Mass per year of pulse one	**Total Mass for Entire Period**	**Total Mass for Entire Period**
	M2 Mass per year of pulse two	**Mean Time of Mass Input** After mass begins to reach the water table	**Mean Time of Mass Input** After mass begins to reach the water table
	M3 Mass per year of pulse three	**Variance in Time of the Distribution of Mass** Around the time of mean mass Input	**Variance in Time of the Distribution of Mass** Around the time of mean mass input

Stake Holder Estimate of the Mass Distribution

A stake holder suggested relative amounts of mass for each year based on industrial activity at the proposed site. To represent this as a distribution, the relative values of the mass are used in conjunction with a multiplier for adjusting and estimating the total mass entering the system. If one assumes a source timing of 20 years and a mass of 29000 lbs, the resulting distribution is as shown (Figure 5.1).

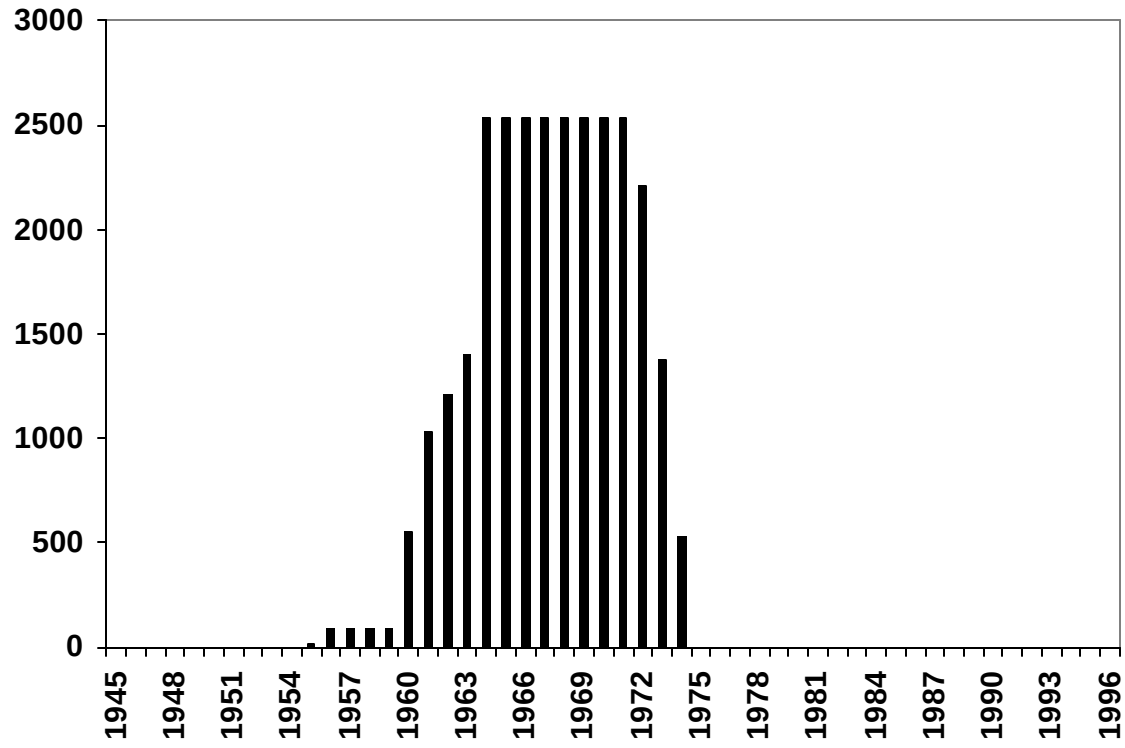

Figure 5.1: Stake Holder mass distribution.

Step Function

The step function provides the ability to define three periods of differing source intensity. Three pulses are chosen that coincide with periods of differing industrial production contracts for the source site. The step function is created such that the starting time and mass are allowed to vary, but the duration of each period is fixed. Hence, the distribution is shown for a start time of 1955. The first pulse occurs for 13 years, the second for 3 years, and the third pulse for 5 years (Figure 5.2).

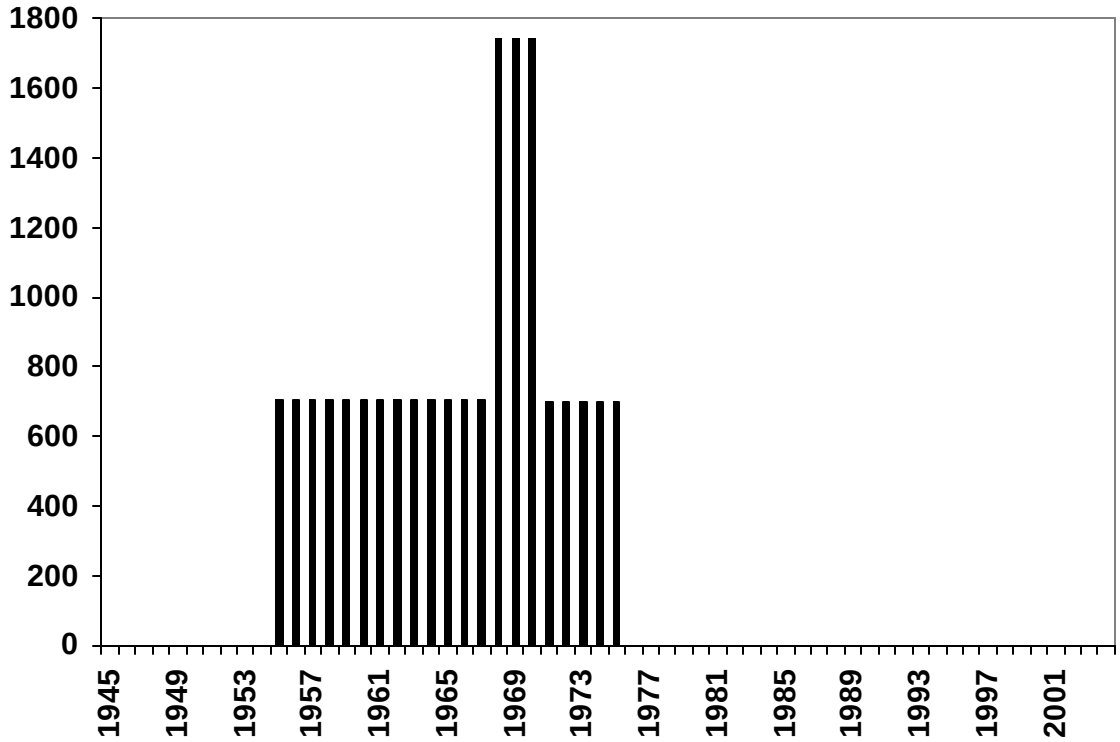

Figure 5.2: Mass distribution represented by the step function.

Truncated Normal Distribution

A normal distribution is described as:

$$f(x) = \frac{mass}{\sqrt{2p\,s^2}} \exp(-(x-m)^2 / 2s^2) \qquad (5.1)$$

where *mass* is the total mass of contaminant introduced at the water table, m is the mean time of mass input relative to the time that mass begins to reach the water table, and s^2 is the variance of the distribution of mass around the time of mean mass input. For input to the transport model, the function is truncated to constrain the period of mass input to 20 years (the duration of industrial activity) so resultant mass distribution is found by normalizing the 20 year portion of the distribution with respect to the maximum value in those years and multiplying by the total mass (see Appendix B for more detail). This function represents a ramping up and down of mass over time. Changes in the mean time of release and variance result in various distributions, such that more mass may enter the system early, late, or in the middle, of the period of industrial activity. Assuming a total mass of 30000 lbs, Figure 5.3 illustrates the flexibility of the function to provide different input distributions.

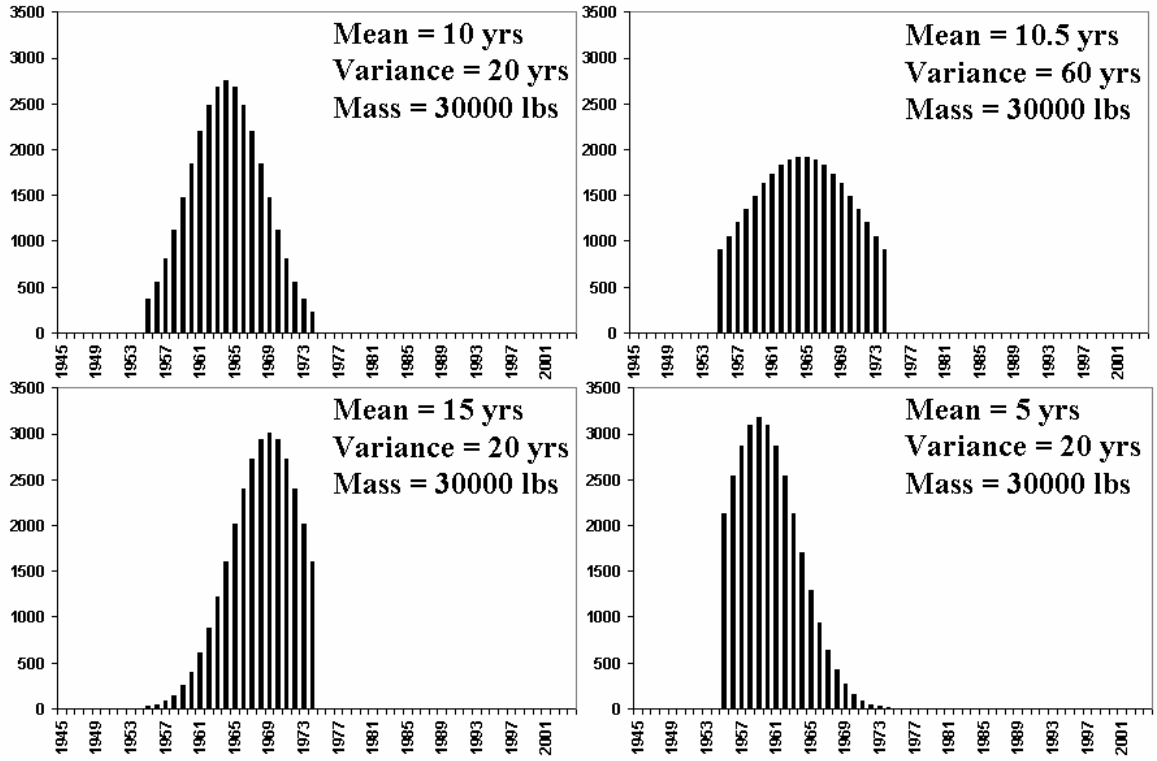

Figure 5.3: Truncated normal distributions represented by mean and variance combinations.

Truncated Lognormal Distribution

A lognormal distribution is described as:

$$f(x) = \frac{mass}{x\sqrt{2p\,s^2}}\exp(-(\ln(x) - m)^2 / 2s^2) \qquad (5.2)$$

where *mass* is the total mass of contaminant introduced at the water table, m is the mean time of mass input relative to the time that mass begins to reach the water table, and s^2 is the variance of the distribution of mass around the time of mean mass input. For input to the transport model, the function is truncated to constrain the period of mass input to 20 years (the duration of industrial activity) so resultant mass distribution is found by normalizing the 20 year portion of the distribution with respect to the maximum value in those years and multiplying by the total mass (see Appendix B for more detail). However, unlike the truncated normal distribution the truncated lognormal distribution allows for an early or late tail of mass input. Changes in the mean and variance result in different distributions as shown in Figure 5.4.

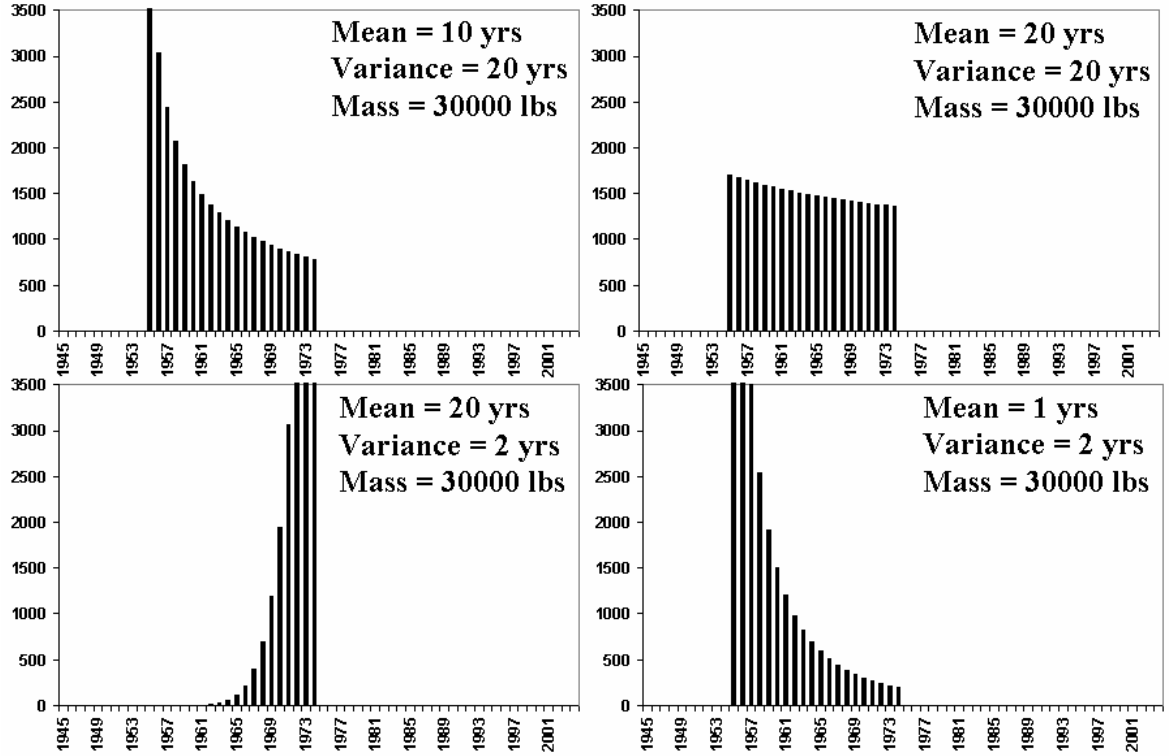

Figure 5.4: Truncated lognormal distributions represented by various mean and variance combinations.

Results of Estimating Transport Parameters for Alternative Conceptual Models

Before presenting the results, it is important to note that some constraints were applied to the regression work for this thesis. Constraining a regression is not desirable if the optimized values are equal to a constraint. This occurred in a few cases and is viewed as a shortcoming of this thesis that can be improved upon in future work. One constraint of concern is the lower bound on the time after the start of the flow simulation that mass first reaches the water table. This constraint was set at 10 years (1955) because TCE was not used before that time. That is, the lower bound of "source timing" was set at 10 years and for one case this was the optimal value. The other constraint selected as an optimal value was the lower bound for longitudinal dispersivity. This was limited to 410 feet in order to maintain a Peclet number of 1.0 or less. A somewhat larger value, two or so, would be acceptable and in the future the regression should be repeated without this constraint.

Regression statistics show the most representative source function is the normalized truncated lognormal function (Table 5.2). However, some estimates reached bounds that should not have been included in the regression, or became insensitive during the regression and so were omitted from the estimation procedure and so should be viewed as specified rather than estimated parameters. For instance, inversion results showed that the mean arrival time and variance of timing of the truncated lognormal function had no sensitivity at the end of the regression. The source timing for both the stake holder and

the truncated normal functions showed insensitivity. Finally, the estimates of the source timing for the step function occurred at the lower bounded value, in conjunction with both masses of pulse one and two showing no sensitivity. Consequently, for further evaluation in this thesis these are treated as specified parameter values.

Table 5.2: Regression statistics for each of the contaminant source functions.

SOURCE FUNCTION	SOSWR	CEV Lower 95%	CEV	CEV Upper 95%
Truncated Lognormal	167.3	0.5873	0.6105	0.8406
Stake Holder	178.2	0.6258	0.6481	0.8957
Truncated Normal	179.4	0.6299	0.6595	0.9015
Step Function	307.9	1.081	1.1238	1.5475

The mass and time coordinates of the centroid of the source distribution are calculated to provide a summary measure of the estimated distributions. Examples are provided in Figure 5.5 to illustrate how calculation of the centroid depicts timing and magnitude of mass entering the ground water system. Final parameter values and the time and mass coordinates of the source distribution for each conceptual model are presented in Table 5.3. Note that for the step function the total mass is shown instead of the estimated mass for each pulse. Given that in some cases parameters were omitted from the regression, those values are treated as if they had been specified rather than estimated.

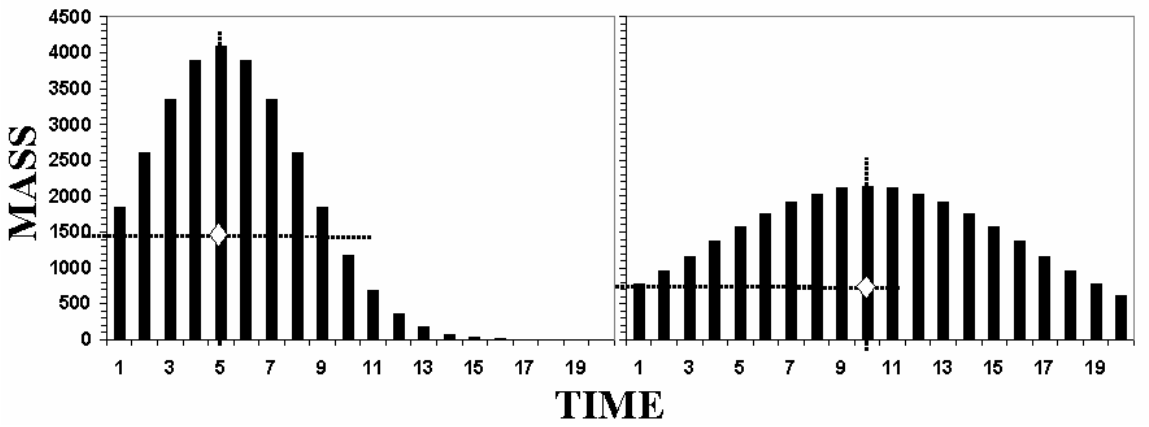

Figure 5.5: Example showing how the mass and time coordinates of the centroid of mass reaching the ground water table summarizes the character of the source distribution.

Table 5.3: Optimized parameter values, and time and mass coordinates of the centroids for each optimized model. Gray shaded cells represent parameters that were insensitive at the end of the regression. Darker gray cells indicate parameters that reached a specified bound and so were not estimated.

Source Function	Dispersivity (ft)	Source Timing (years)	Mass (lbs)	Mean Time of Release (year)	Variance of Timing ($year^2$)	Time Centroid (year)	Mass Centroid (lbs)
Lognormal	410	29	18200	3.2	55.4	1979	659
Stake Holder	410	20	14860			1976	509
Normal	459	17	14020	15.4	12.5	1975	604
Step Function	479	10	5033			1972	438

The normalized truncated lognormal model has the most representative regression statistics of the group depicted in each of the calibration quality graphics: 1) weighted residuals versus simulated equivalents (Figure 5.6); 2) weighted observed values versus weighted simulated equivalents (Figure 5.7); and 3) probability versus ordered weighted residuals (Figure 5.8). None of the weighted residuals versus standard normal statistics form a straight line, so the comparison with uncorrelated and correlated random normal

deviates is completed for each. Similar deviations from the weighted residuals are apparent for the independent (uncorrelated) and correlated random numbers with respect to the normalized truncated lognormal, normalized truncated normal, and stake holder functions, with the closest resemblance to the weighted residuals for the normalized truncated lognormal function. The step function is least representative conceptual model. The pattern of positive and negative residuals is similar for the normalized truncated lognormal, normalized truncated normal, and stake holder conceptualizations with a combination of both positive and negative residuals in space. However, the step function is again an exception with a biased distribution of positive residuals (Figure 5.9).

The plumes, as simulated with the optimal estimated parameters, are contoured for each conceptual model and compared with the 0.5ppb contour line of the observed field concentrations (Figure 5.10). As can be seen, the plumes simulated using the normalized truncated lognormal, normalized truncated normal, and stake holder functions have the closest resemblance to the field plume, with the normalized truncated lognormal function giving the best representation. Once again, the step function is the least representative of the group.

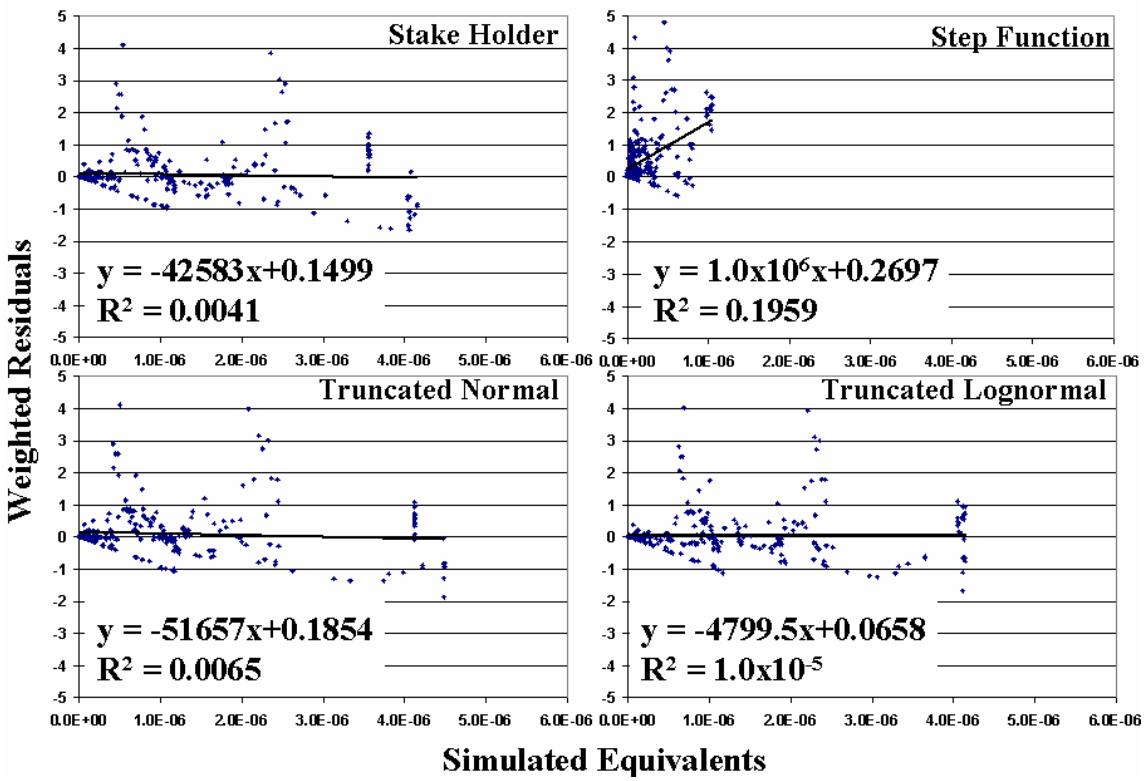

Figure 5.6: Weighted residuals versus simulated equivalents for the alternative models. A "perfect" fit would have y=0x+0, y=0.

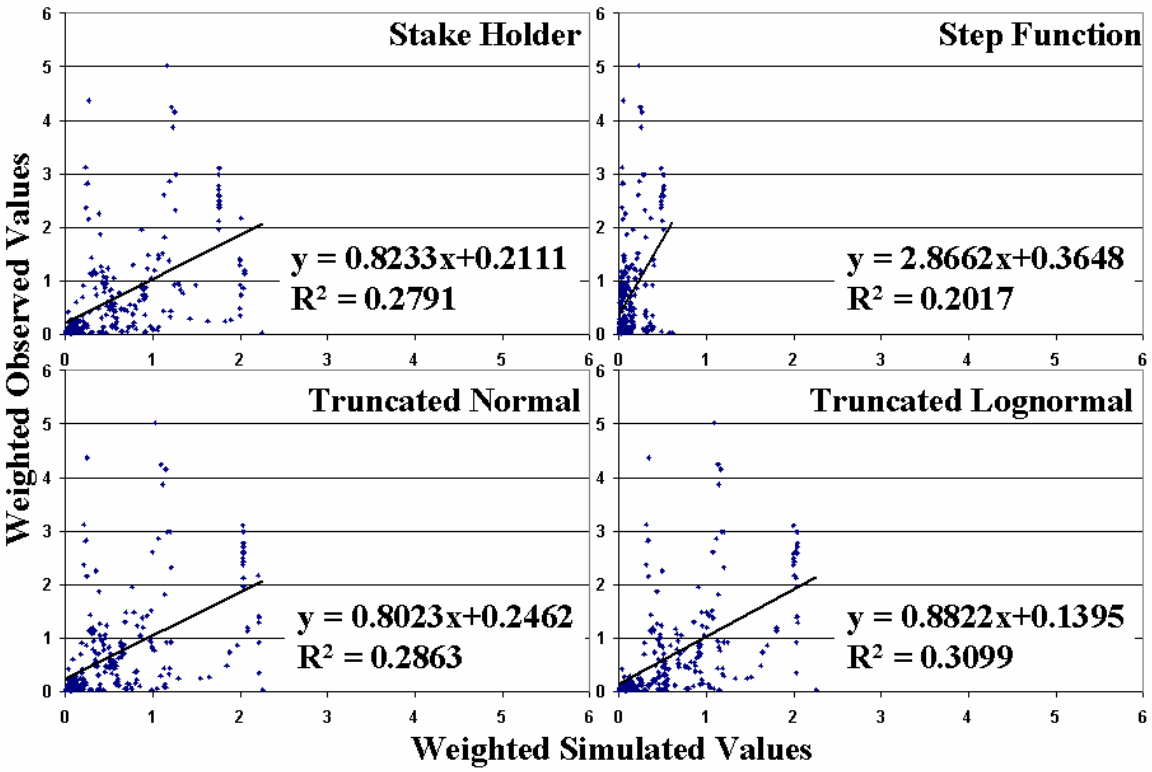

Figure 5.7: Weighted observed values versus weighted simulated values for the alternative models. A perfect model would have y=1x+0, y=x.

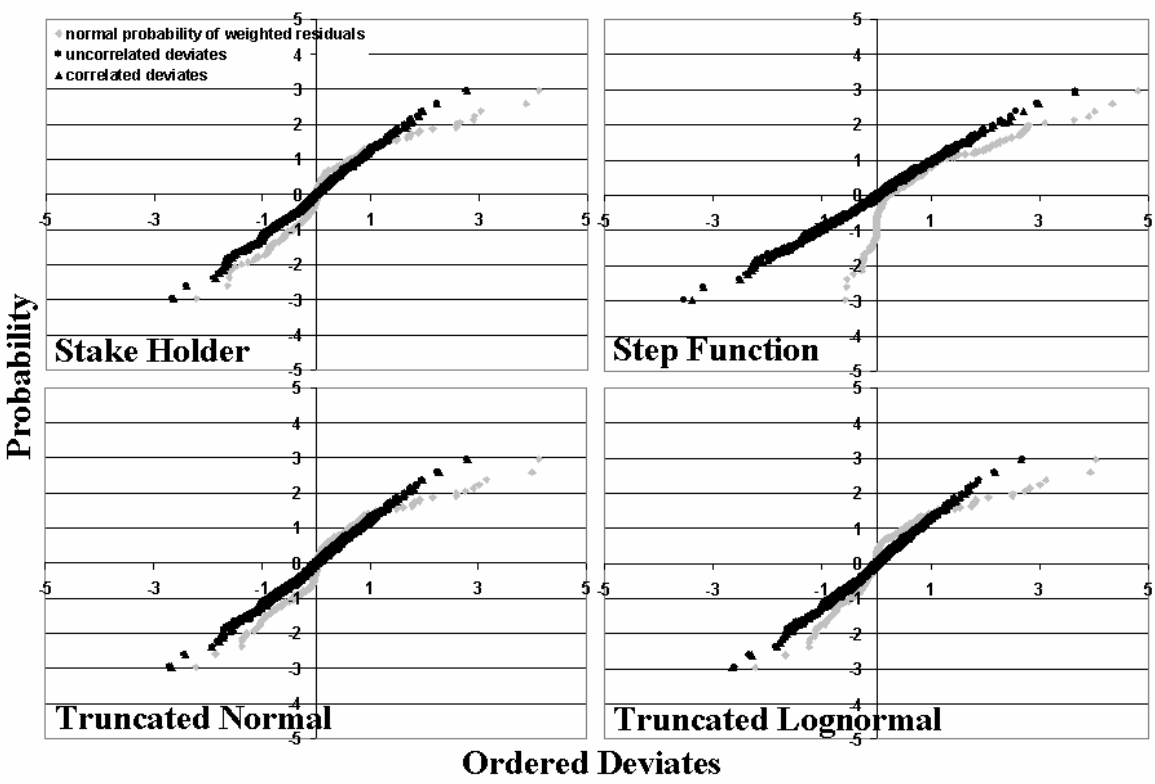

Figure 5.8: Normal probability graph showing trend of weighted residuals, uncorrelated and correlated deviates for the conceptual models. A perfect model would have values matching the shape of the correlated residuals.

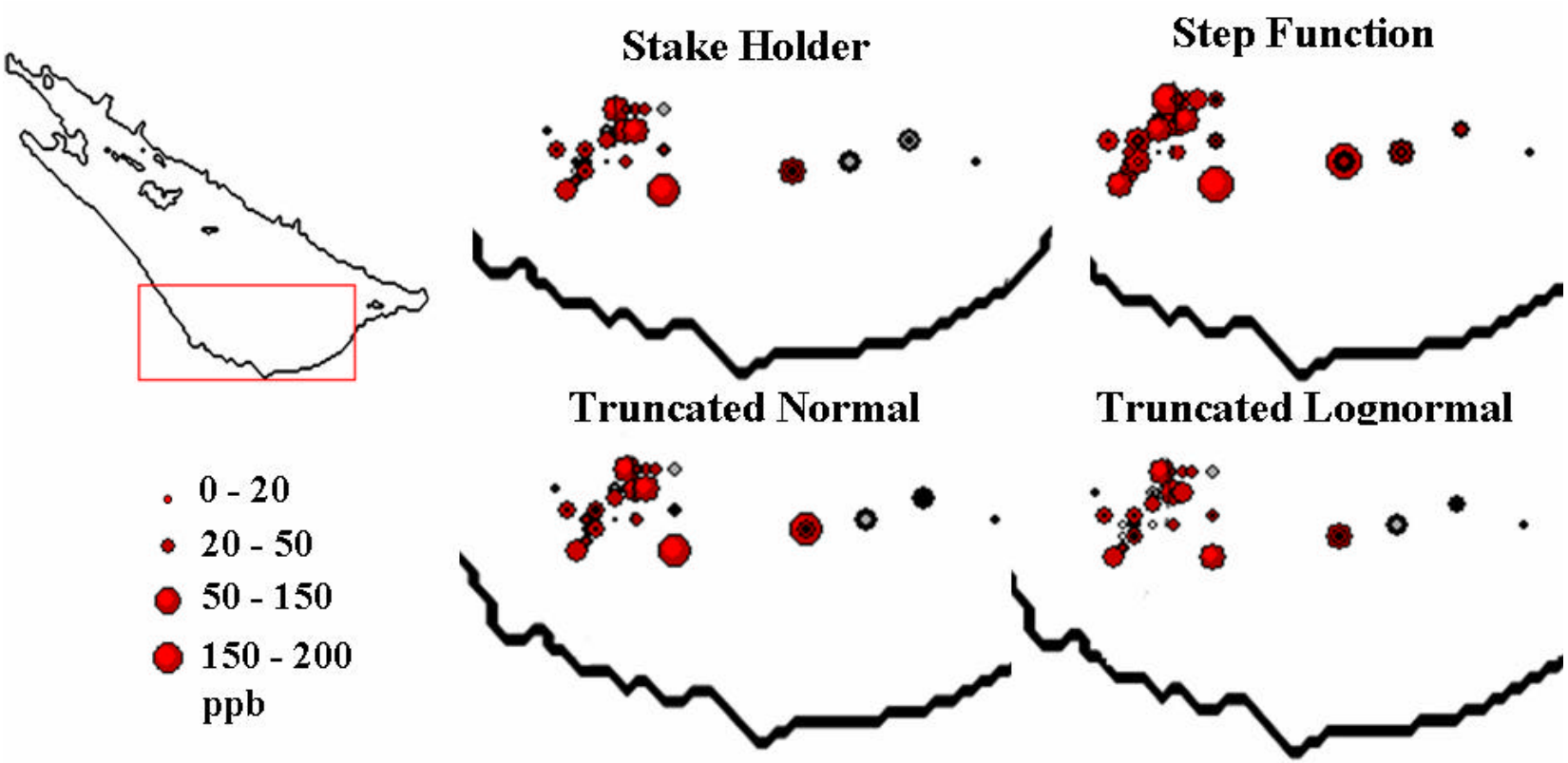

Figure 5.9: Spatial distribution of concentration residuals for all times for the conceptual models.

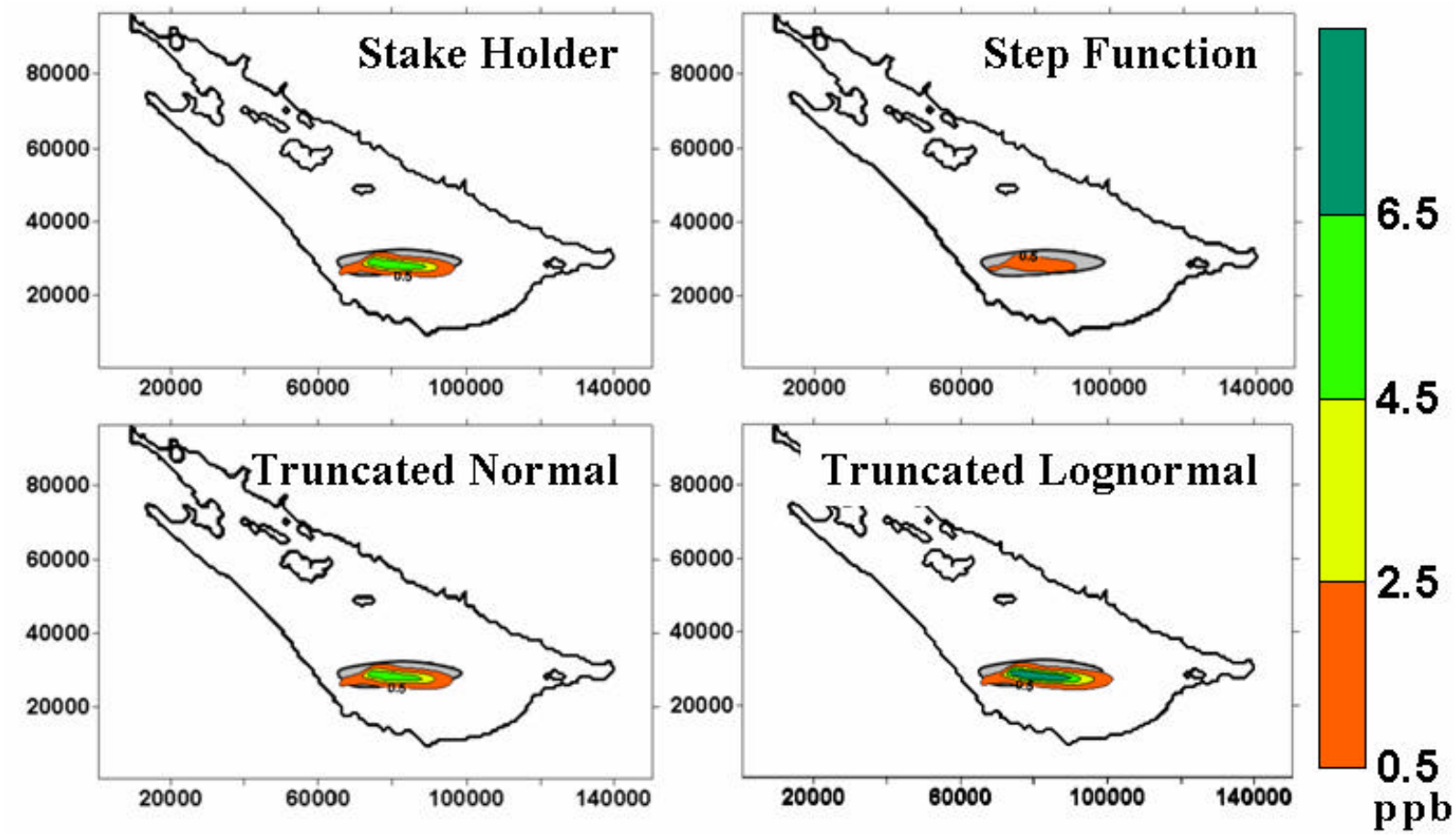

Figure 5.10: Contaminant plumes with respect to the final parameters for each of the conceptual models. Underlying plume (gray) represents the 0.5ppb contour line of the observed concentration data.

Verifying Unique Optimal Parameter Values

To confirm the uniqueness of optimized values for the normalized truncated lognormal function (Table 5.3) we use the methodology discussed in Chapter 4. For this, testing the constraint on the lower bound of dispersivity was removed. However, a constraint that did not affect results before, does affect these results. The code that calculates the normalized truncated lognormal distribution will fail if the variance exceeds 60 years.[2] Sixty was specified as an upper bound and all of the regressions reached the upper bound. It is expected that this is compensating for the lower estimated value of dispersivity by spreading the course, suggesting we may not be able to independently estimate these values and this should be explored in future work.

None of the regressions converged for the alternative starting parameters used for uniqueness test. However, the final values of dispersivity, source timing, and mass are similar suggesting the non-uniqueness is not extreme. Estimates of the mean and variance are also similar, but are more uncertain as reflected by the larger confidence intervals. The starting parameter values for each run, final estimated parameter values, and the SOSWR with respect to each uniqueness-testing regression are listed in Table 5.4. Results of the uniqueness test are depicted in Figures 5.11, 5.12, and 5.13 showing final parameter values and their upper and lower 95% linear confidence intervals.

Table 5.4: Initial and final parameter values for three regressions. Note that shaded cells represent parameters that were omitted during regression due to reaching the upper bound for variance in the code that calculates the source function.

Parameters	Initial Values Run 1	Final	Initial Values Run 2	Final	Initial Values Run 3	Final
Dispersivity	100	**316**	600	**327**	500	**314**
Source Timing	15	**28.1**	19.5	**28.0**	30	**28.2**
Mass	15000	**18700**	30000	**19090**	17904	**18680**
Mean	5	**9**	20	**13**	10	**9**
Variance	10	**60**	30	**60**	15	**60**
SOSWR		**166.8**		**166.7**		**166.8**

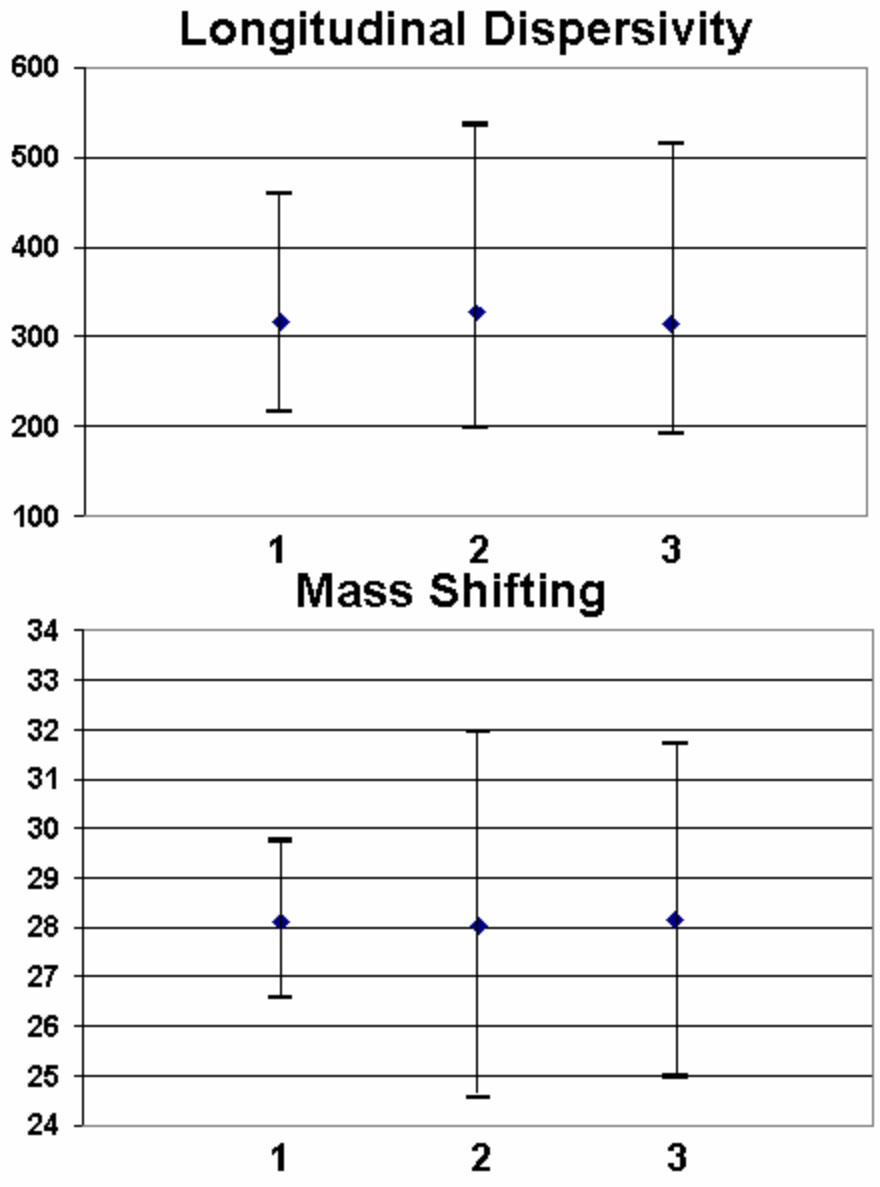

Figure 5.11: Optimal parameter values and their upper and lower 95% confidence intervals for three regression runs. Diamonds are the optimal values and error bars represent the upper and lower linear 95% confidence intervals. Ideally all diamonds should fall within half of the adjacent point's error bars.

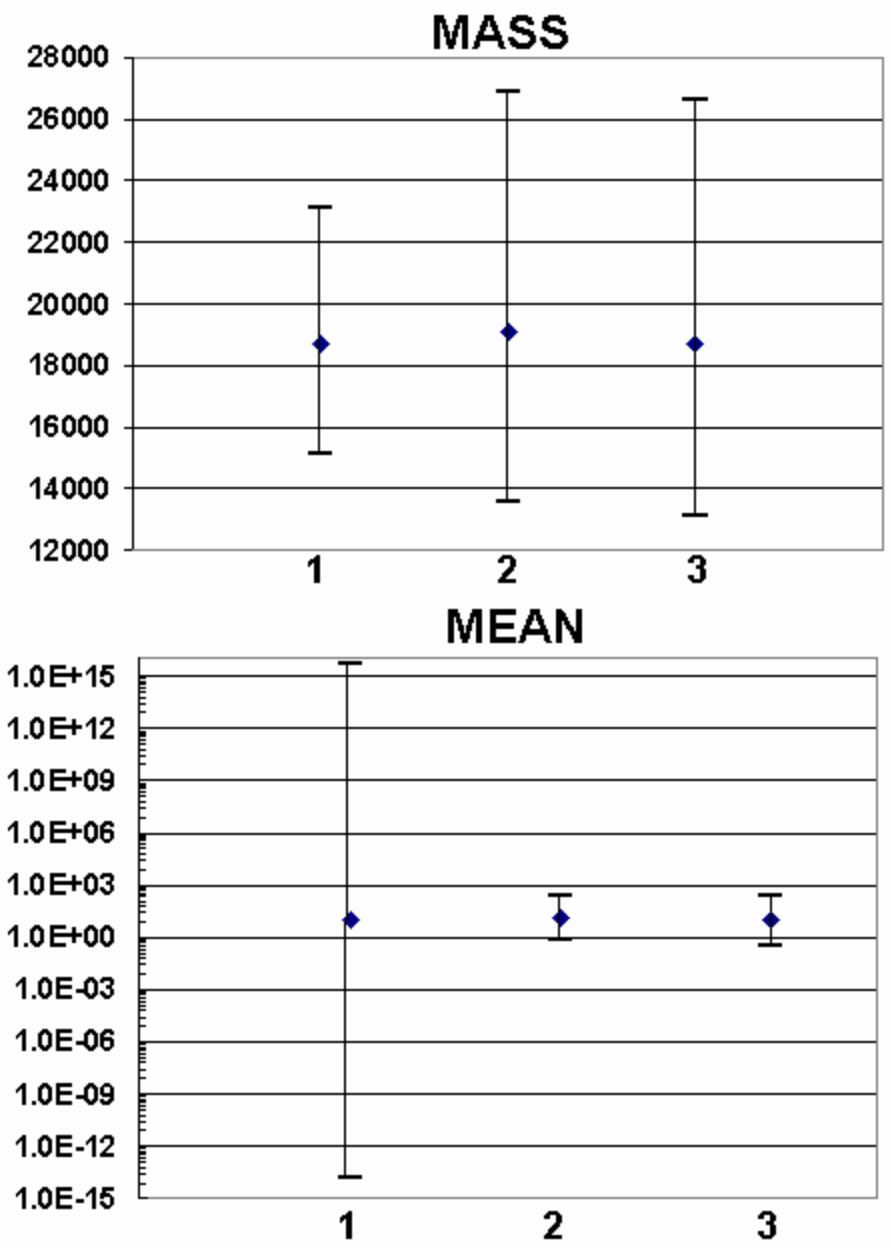

Figure 5.12: Optimal parameter values and their upper and lower 95% confidence intervals for three regression runs. Diamonds are the optimal values and error bars represent the upper and lower linear 95% confidence intervals. Ideally all diamonds should fall within half of the adjacent point's error bars.

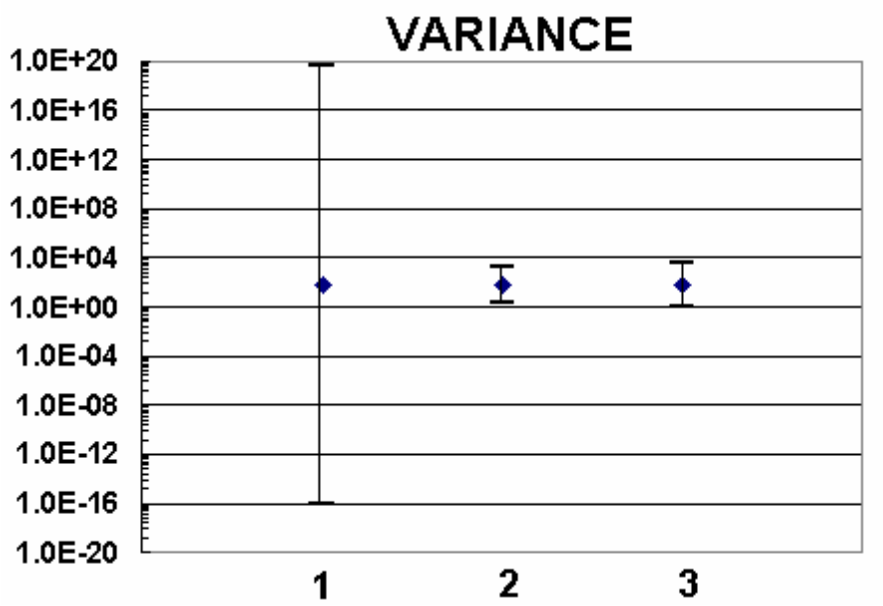

Figure 5.13: Optimal parameter values and their upper and lower 95% confidence intervals for three regression runs. Diamonds are the optimal values and error bars represent the upper and lower linear 95% confidence intervals. Ideally all diamonds should fall within half of the adjacent point's error bars.

The overlapping confidence intervals suggest that the parameters can be independently estimated (i.e., there is a unique solution for the regression). However, the SOSWR is approximately 160 for many sets of parameter values making it difficult to obtain convergence of the regression, which can be seen when depicting the time and mass coordinates of the centroids of the source distributions with their associated SOSWR values (Figure 5.14). Clearly the objective function is flat, likely due to large error in the observations or correlation between multiple parameters. The SOSWR surface may have a global minimum that was not found by the regression. However, derivative based parameter estimation techniques that invoke perturbation techniques (such as

UCODE_2005, MODFLOW-PES, and PEST), may not be robust enough to find the minimum. The global minimum may occur for an earlier time and a smaller mass (Figure 5.15).

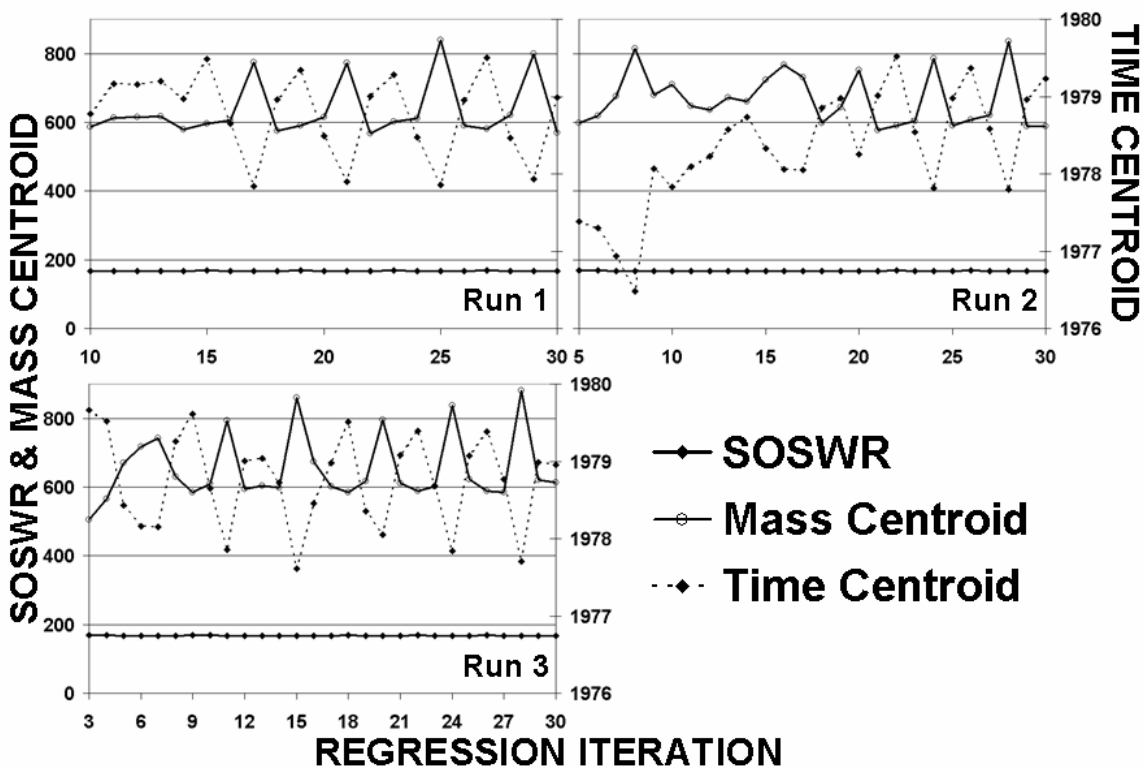

Figure 5.14: Variation of the time and mass coordinates of centroid of the source distributions with respect to SOSWR values for the three regressions using the modified truncated lognormal function.

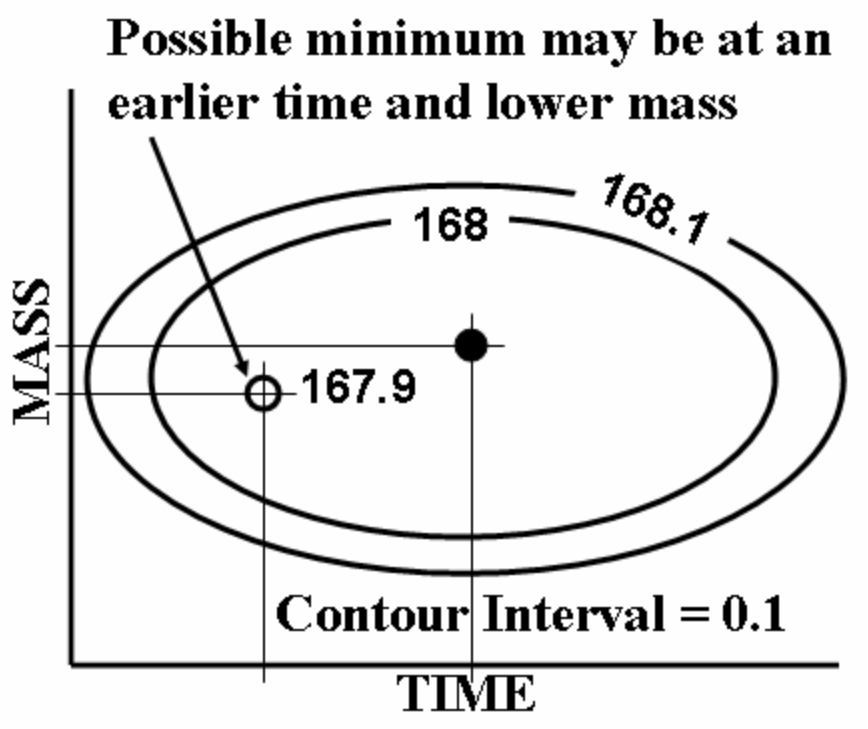

Figure 5.15: Concept of a flat SOSWR surface containing a global minimum.

Model Weighting

Although the results suggest the source distribution is yet to be determined, for the sake of this thesis and to illustrate the technique, model averaging is undertaken.

Multi-model averaging integrates results from alternative models of a system based on weights that reflect relative information content of models in a set. Multi-model averaging provides a more realistic measure of precision than evaluation of any one model. Here we use the enhanced Akaike's Information Criterion (AICc) for weighting models which reflects information lost when the full truth is approximated by a given model:

$$AICc = n\log(s^2) + 2k + \left[\frac{2k(k+1)}{n-k-1}\right] \qquad (5.3)$$

where s^2 is the estimated residual variance (the quotient of the sum of squared weighted residuals and the number of observations, SOSWR/n), n is the number of observations, and k is the number of estimated parameters for the model (plus one because s^2 is considered to be estimated). AICc is based on Kullback-Leibler (KL) information which provides a rigorous foundation for model inference that is simple to compute, easy to interpret, and selects parsimonious models.

Delta values, $\Delta_i = AICc_i - AICc_{\min}$, describe information loss on a log scale (Poeter and Anderson, 2005) and are used to calculate model weights that sum to one for a given

set of models, where $AICc_{min}$ is the minimum AICc value of all the models in the set. The weight of evidence in favor of each model in the set is:

$$w_i = \frac{\exp^{-0.5\Delta_i}}{\sum_{j=1}^{R} \exp^{-0.5\Delta j}} \qquad (5.4)$$

where w_i is the weight of evidence in favor of model i being the best model in the sense of minimum KL information loss and R is the set of all models (Poeter and Anderson, 2005).

Model Averaging Results

Weights for each model are dependent on the number of observations, number of estimated parameters, and SOSWR. For the set of alternative conceptual models considered, the model weights indicate the truncated lognormal function is most representative of the source history (Table 5.5). The final mass distributions through time for each conceptual model are depicted in Figure 5.16.

Table 5.5: Model weights for alternative source functions.

Source Function	n	k	SOSWR	AICc	Model Weight
Truncated Lognormal	276	3	167.3	-53.9	0.94
Stake Holder	276	2	178.2	-48.4	0.058
Truncated Normal	276	5	179.4	-41.4	0.0018
Step Function	276	3	307.9	19.2	1.2×10^{-16}

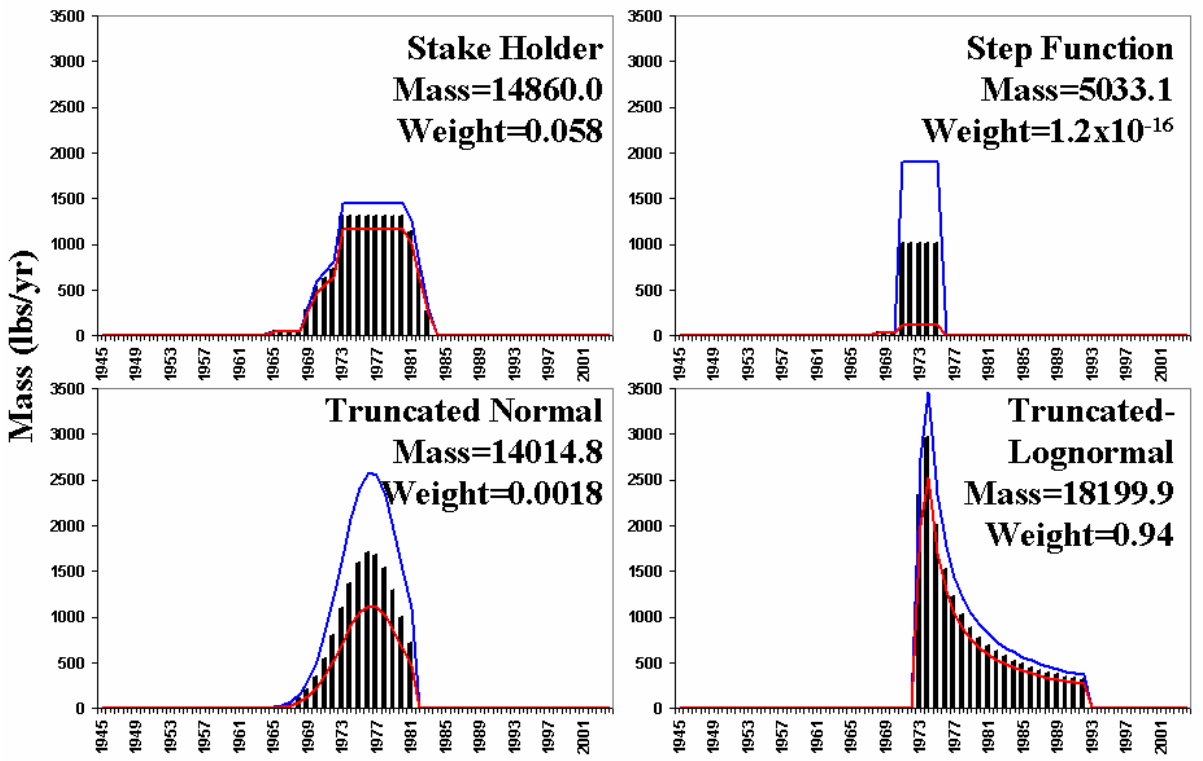

Figure 5.16: Contaminant source functions representing time versus mass in lbs/yr over a sixty year timeframe from 1945 to 2004. Blue lines represent the upper 95% confidence interval and red lines represent the lower interval.

The model weights and their mass distributions are used to generate the average mass input estimated by all four conceptual models. To do this, the mass for each year of each conceptual model is multiplied by its respective weight and then summed. The modified truncated lognormal function has a substantially higher weight than the alternatives, consequently, the average distribution looks much like that distribution (Figure 5.17). Given this limited set of models and the uncertainty described above, the time when most of the mass reached the ground-water table cannot be determined at this time.

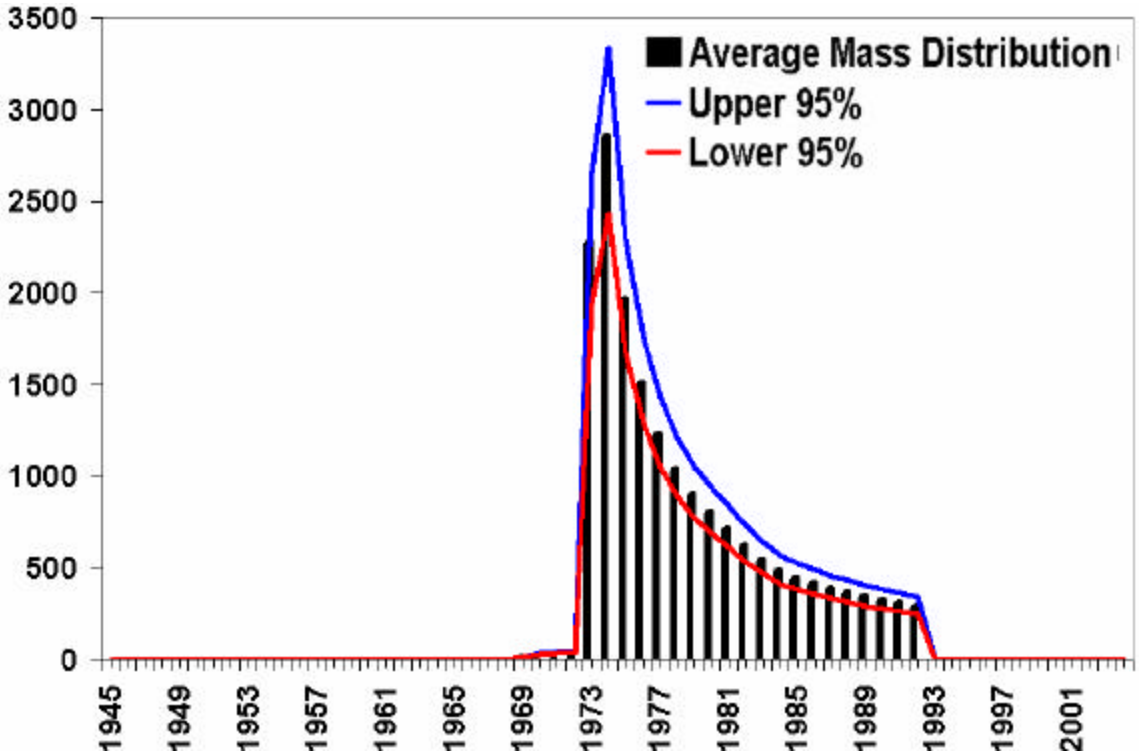

Figure 5.17: Average mass distribution derived from model averaging the conceptual models. Blue and red lines are the upper and lower averaged 95% confidence intervals.

CHAPTER 6: CONCLUSIONS AND FUTURE WORK

Conclusions

When calibrating a ground-water contaminant transport model, it is common practice to substitute fabricated values for censored data, e.g., detection limit, one-half the detection limit, or zero. However, we only know that the value is less than the detection limit. This is taken into account by the censored-residual approach, which is shown to produce more representative models. For instance, when using the censored-residual approach the synthetic examples show a better fit to field observations and estimated parameter values are closer to true values used to generate the synthetic models. Given that the censored-residual approach resulted in the best fit to synthetic data and more representative parameter values for the synthetic test cases, we infer that it produces the most representative parameter values for field cases as well.

As mentioned previously, models cannot entirely represent all the subtleties of ground-water system, as they are only mere approximations of nature. For instance, reasonable alternative models of a system can yield similar calibrations and yet provide substantially different results. Evaluation of alternative models indicates uncertainty associated with one model is small compared with the uncertainty reflected by multiple conceptual models. Hence, various conceptual models which represent possible

conditions/scenarios need to be developed, calibrated, used to make predictions, and their average results reported.

A modified truncated lognormal source distribution is most representative of the TCE plume in Bunker Hill basin. However, only four source functions are considered and the modified truncated lognormal model is non-unique either due to large error in observations, correlation of parameters, and/or an inadequate conceptual model. Given this limited set of models and the non-unique solution of the most representative model, further work is needed to determine the distribution of mass arrival at the water table.

Future Work

Because the timing of mass arrival at the water table cannot be determined from this analysis, several future tasks are appropriate. Calibration of the flow model should be reconsidered to assure a representative flow field. Non-uniqueness of the flow model should also be evaluated. Next, only four source functions are evaluated, which may not provide adequate flexibility in representing the source. Hence, more conceptual models of the source should be developed. Perhaps evaluation of concentration time-series in observation wells would provide insight on alternative distributions. The concentration observations need to be reanalyzed to reevaluate their accuracy. It may be appropriate to use similar weights for censored and uncensored observations, as this may better represent the spatial distribution of the plume. In addition, it may be useful to remove the

concentration observations derived from purveyor wells, as observations from monitor wells may produce a more representative data set. Lastly, alternative parameter estimation schemes can also be invoked such as genetic algorithms, shuffled complex evolution, function approximation, or other methods.

REFERENCES

Alapati, S., and Kabala, K. J., 2000, Recovering the release history of a groundwater contaminant using a non-linear least-squares method, Hydrol. Processes, 14, 1003-1016.

Anderson, D., 2003, Multimodel Inference Based on Kullback-Leibler Information, MODFLOW and More 2003: Understanding through Modeling, Conference Proceedings.

Atmadja, J., Bagtzoglou, A, 2001, State of the Art Report on Mathematical Methods for Groundwater Pollution Source Identification, Environmental Forensics, 2, 205-214.

Atmadja, J., Bagtzoglou, A, 2001, Pollution source identification in heterogeneous media, Water Resources Research, Vol. 37, No. 8.

Burnham, K. P., and D. R. Anderson. 2002, Model selection and multi-model inference: a practical information-theoretic approach. Springer-Verlag, New York, NY.

Carrera, J., and Neuman, P., 1986, Estimation of Aquifer Parameters Under Transient and Steady State Conditions: 1. Maximum Likelihood Method Incorporating Prior Information, Water Resources Research, Vol. 22, No. 2.

Chongxuan, L., and Ball, W., 1999, Application of inverse methods to contaminant source identification from aquitard diffusion profiles at Dover AFB, Delaware, Water Resources Research, Vol. 35, No. 7.

Danskin, W., 2006, Hydrology, Description of Computer Models, and Evaluation of Selected Water-Management Alternatives in the San Bernardino Area, California, USGS Open File Report 2005-1278.

Danskin, Wes, personal communication, 2006, USGS.

Dutcher, L., and Garrett, A, 1963, Geologic and hydrologic features of the San Bernardino area California, with special reference to underflow across the San Jacinto fault, USGS Water Supply Paper 1419.

Domenico, P., and Schwartz, F., 1990, Physical and Chemical Hydrogeology, John Wiley & Sons, Inc.

Eckis, R., 1934, Geology and Groundwater Storage Capacity of Valley Fill, South Coastal Basin Investigations, State of California Department of Public Works, Division of Water Resources, Bulletin No. 45.

EIR, 2004, Community Report and Draft Environmental Impact Report for the Santa Ana River Water Right Applications for Supplemental Water Supply, October 2004, http://www.sbvmwd.com/

Essaid et al., 2003, Inverse modeling of BTEX dissolution and biodegradation at the Bemidji, MN crude-oil spill site, Journal of Contaminant Hydrology, 67.

Gilliom, R., and Helsel, D., 1986, Estimation of Distributional Parameters for Censored Trace Level Water Quality Data 1. Estimation Techniques, Water Resources Research, Vol. 22, No. 2.

Gorelick et al., 1983, Identifying Sources of Groundwater Pollution: An Optimization Approach, Water Resources Research, Vol 19., No. 13.

Harbaugh, A.W., et al., 1996, User's Documentation for MODFLOW-96, an update to the US Geological Survey Modular Finite-Difference Ground-Water Flow Model: U.S. Geological Survey Open-File Report 96-485.

Harbaugh, A.W., et al., 2000, MODFLOW-2000, the U.S. Geological Survey modular ground-water model, User's guide to the Modularization concepts and the Ground-Water Flow Process: U.S. Geological Survey Open-File Report 00-92, 121p.

Hardt, W., and Hutchinson, C., 1980, Development and use of a mathematical model of the San Bernardino Valley ground-water basin, California, U.S. Geological Survey Open-File Report 80-576

Helsel, D., 2005, Nondetects and data analysis: statistics for censored environmental data, John Wiley & Sons

Helsel, D., 2005, More Than Obvious: Better methods for interpreting nondetect data, Environmental Science and Technology, Vol 39, No. 20, pp 419A-423A.

Hill, M., 1998, Methods and Guidelines for Effective Model Calibration, U.S. Geological Survey Water-Resources Investigations Report 98-4005

Hill, M.C. and Tiedeman, Effective groundwater model calibration, with analysis of sensitivities, predictions, and uncertainty: Wiley and Sons, New York, New York, in press for 2007.

Hojberg, A., and Refsgaard, J., 2005, parameter uncertainty versus conceptual models, Water Science and Technology, Vol 52, No. 6, pp 177-186.

HSI, 1998, Redlands Groundwater Modeling Project; Groundwater Flow and TCE Modeling Documentation Report., HSI GeoTrans.

Lowell, W. et al., 1988, Appraisal of Ground-Water Quality in the Bunker Hill Basin of San Bernardino Valley, California, U.S. Geological Survey Water-Resources Investigation Report 88-4203

Mahar, P., and Datta, B., 2000, Identification of Pollution Sources in Transient Groundwater Systems, Water Resources Management, 14.

Medina, A., and Carrera, J., 1996, Coupled estimation of flow and solute transport parameters, Water Resources Research, Vol 32., No. 10.

Michalak, A., and Kitanidis, P., 2004, Estimation of historical groundwater contaminant distribution using the adjoint method applied to geostatistical inverse modeling, Water Resources Research, Vol. 40, W08302.

Montgomery, J.H., and Welkom, L.M., 1990, Groudwater Chemicals Desk Reference, Lewis Publishers Inc., Chelsea, Michigan.

Neupauer et al., 2000, Comparison of inverse methods for reconstructing the release history of a groundwater contamination source, Water Resources Research, Vol. 36, No. 9.

Neupauer, R, and Wilson, J., 1999, Adjoint method for obtaining backward-in-time location and travel time probabilities of a conservative groundwater contaminant, Water Resources Research, Vol. 35, No. 11.

Neupauer, R, and Wilson, J., 2001, Adjoint-derived location and travel time probabilities for a multidimensional groundwater system, Water Resources Research, Vol. 37, No. 6.

Neupauer, R, and Wilson, J., 2002, Backward probabilistic model of groundwater contamination in non-uniform and transient flow, Advances in Water Resources, 25.

Neupauer, R, and Wilson, J., 2004, Numerical Implementation of a Backward Probabilistic Model of Ground Water Contamination, Ground Water, Vol. 42, No. 2.

Personal Communication, 2006, Discussion with Dr. Wes Danskin in regards to realistic values of stream flow that can be added to the Zanja Ditch.

Poeter, E., and Anderson, D., 2005, Multimodel Ranking and Inference in Ground Water Modeling, Ground Water, Vol. 43, No. 4.

Poeter, E., and Hill, M., 1997, Inverse Models: A Necessary Next Step in Ground-Water Modeling, Ground Water, Vol. 35, No. 2.

Poeter, E. et al., 2005, UCODE_2005 and Six Other Computer Codes for Universal Sensitivity Analysis, Calibration, and Uncertainty Evaluation, U.S. Geological Survey, Techniques and Methods 6-A11., http://water.usgs.gov/software/ucode.html/

Parker, J., and Islam, M., 2000, Inverse modeling to estimate LNAPL plume release Timing, Journal of Contaminant Hydrology, 45.

Sonnenborg, O. et al., 1996, Contaminant transport at a waste residue deposit 1. Inverse flow and nonreactive transport modeling, Water Resources Research, Vol. 32, No. 4.

Snodgrass, M., and Kitanidis, P., 1997, A geostatistical approach to contaminant source identification, Water Resources Research, Vol, 33, No. 4.

SBVMWD, 2004, San Bernardino Valley Municipal Water District, August 2004, SCH No. 2003121150

Skaggs, T., and Kabala, Z., 1994, Recovering the release history of a groundwater contaminant, Water Resources Research, Vol. 30, No. 1.

Skaggs, T., and Kabala, Z., 1995, Recovering the history of a groundwater contaminant plume: Method of quasi-reversibility, Water Resources Research, Vol. 31, No. 11.

Skaggs, T., and Kabala, Z., 1998, Limitations in recovering the history of a groundwater contaminant plume, Journal of Contaminant Hydrology 33.

Sun, A. et al., 2006, A constrained robust least squares approach for contaminant release history identification, Water Resources Research, Vol. 42, W04414.

Sun, A. et al., 2006, A Robust Framework for Contaminant Source Identification Using MODFLOW/MT3DMS, MODFLOW and More 2006 Conference Proceedings.
Wagner, B., 1992, Simultaneous parameter estimation and contaminant source characterization for coupled groundwater flow and contaminant transport modeling, Journal of Hydrology, 135.

USDA, 1996, United States Department of Agriculture, 1996, Soil Quality Resource Concerns: Compaction, Soil Quality Information Sheet.

Wagner, B., 1992, Simultaneous parameter estimation and contaminant source characterization for coupled groundwater flow and contaminant transport modeling, Journal of Hydrology, 135.

Wagner, B., and Gorelick, S., 1986, A Statistical Methodology for Estimating Transport Parameters: Theory and Applications to One-Dimensional Advective-Dispersive Systems, Water Resources Research, Vol 22., No. 8.

Wagner, B., and Gorelick, S., 1987, Optimal Groundwater Quality Management Under Parameter Uncertainty, Water Resources Research, Vol 23., No. 7.

Zheng, C., and Wang, P., MT3DMS V5 A Modular Three-Dimensional Multispecies Transport Model for Simulation of Contaminants in Groundwater, U.S. Army Corps of Engineers, Version 5.0, 2005

Zheng, C., and Bennett, G., 2002, Applied Contaminant Transport Modeling 2nd Edition, Wiley and Sons, Inc., NY.

APPENDIX A: SOURCE CODES FOR THE CONCEPTUAL MODELS

Each alternative model described in Chapter 5 is coded using the FORTRAN 90 programming language and is located in their respective directories on the compact disk included on the back cover of this report, as are their input and output files.

Truncated Normal Distribution

The truncated normal distribution program is NormalDist.f90. This program outputs two files: 1) a check file that lists the year, mass for that year, and the summation of the total mass input for the entire simulation; and 2) an MT3DMS source-sink mixing package input file that is used by the transport program to simulate the TCE migration. The input file, NormDist.in, controls the parameters of the distribution (Figure A.1). The estimated parameters in this study include mass, mean, variance, and shift. The input item, shift, controls the amount of time that mass can be entered into the aquifer.

```
1              SOURCE LOCATIONS
30000.0D0      MASS
10.0D0         SHIFT
60             Number of MODFLOW Stress Periods
20.D0          Mean
30.D0          Variance
20   1.00      Number of contaminant stress periods that mass will be injected
               into the aquifer, followed by fractional mass in source period.
```

Figure A.1: Input file for the truncated normal distribution code NormalDist.f90. Only the numbers on the left are needed by the code, while the text just explains the purpose of the number.

Truncated Lognormal Distribution

The truncated lognormal distribution program is LogNormal.f90. This program produces output similar to the truncated normal distribution program. The input file, LogNorm.in, has the same structure as NormalDist.in (Figure A.1). However, the final input item (fractional mass in source period) is not used by the truncated lognormal program.

Step Function

The step function program is srcdis.f90. This program produces output similar to the truncated normal distribution program. The input file, srcdis.in, controls the parameters of the distribution (Figure A.2). The estimated parameters for this study are the individual mass inputs and the shift value. The first input value shifts the time when mass begins to enter the ground water. The second input value represents the number of MODFLOW stress periods, and the remaining inputs are the respective duration (in years) and magnitudes for each period.

```
10.D0   SHIFT
60      Number of MODFLOW Stress Periods
13      MASS_1  13 Years of mass input      Mass of pulse 1
3       MASS_2  3 Years of mass input       Mass of pulse 2
5       MASS_3  5 Years of mass input       Mass of pulse 3
```

Figure A.2: Example input file for the step function code srcdis.f90

Stake Holder Distribution

The stake holder distribution is produced by the program StakeHolder.f90, which has the same output format as mentioned previously. The input file, StakeHolder.in, controls the parameters of the distribution (Figure A.3). The first, second, and third input values control the amount of mass, the time when mass is first introduced to the water table, and the number of MODFLOW stress periods. The remaining input values are the mass fraction for each period. Each fraction is multiplied by the original total mass to calculate the mass input for each stress period.

```
17904.D0        Original Total Mass in aquifer
10.0D0          SHIFT
60              Number of MODFLOW Stress Periods
0.00065524      MASS Percent for period 1
0.003069283     MASS Percent for period 2
0.003069283     MASS Percent for period 3
0.003069283     MASS Percent for period 4
0.003069283     MASS Percent for period 5
0.019208884     MASS Percent for period 6
0.035520916     MASS Percent for period 7
0.041762941     MASS Percent for period 8
0.048384316     MASS Percent for period 9
0.087526296     MASS Percent for period 10
0.087526296     MASS Percent for period 11
0.087526296     MASS Percent for period 12
0.087526296     MASS Percent for period 13
0.087526296     MASS Percent for period 14
0.087526296     MASS Percent for period 15
0.087526296     MASS Percent for period 16
0.087526296     MASS Percent for period 17
0.076249267     MASS Percent for period 18
0.047453185     MASS Percent for period 19
0.018277753     MASS Percent for period 20
```

Figure A.3: Example input file for the stakeholder distribution code InitEstimate.f90

APPENDIX B: CONTENTS OF THE COMPACT DISK

The compact disk included with this thesis includes all files and codes required to reproduce the work presented herein.

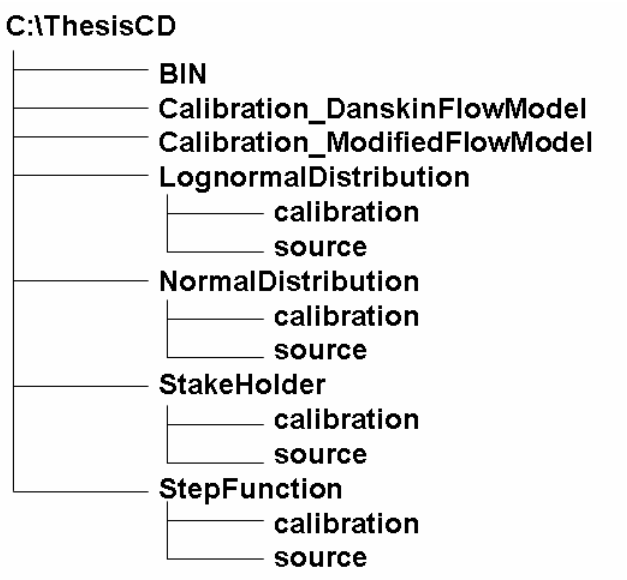

The list above represents the directory structure of the CD contents. Each directory will be discussed individually, as well as, the execution methodology to run the needed applications for model evaluation/calibration. To run the applications from the provided CD without any changes, the directories on the CD have to remain in the same structure when copied, i.e., copy the ThesisCD contents to the C drive of the respective computer. If the desired location is not C:\ThesisCD, then the paths for each batch file will have to be changed. This will be discussed in the explanations of batch files below.

Calibration_DanskinFlowModel Directory

The Calibration_DanskinFlowModel directory contains the Danskin (2006) original flow model in MODFLOW-2000 format and the input, batch, executable, and output files used and generated during the model evaluation. The batch files used to run the applications for the original Danskin model evaluation are RunApps.bat as follows:

```
@echo off
:: Change the ungaged recharge
echo *** UPDATING THE UNGAGED RECHAGE ***
C:\ThesisCD\BIN\Factor.exe

echo *** RUNNING DANSKIN'S SPECIALIZED MODFLOW-2000 ***
C:\ThesisCD\BIN\WesMF2K.exe Danskin.nam

echo *** CALCULATE THE STREAMFLOW LEAKAGE ***
find "STREAM LEAKAGE =" 2k.lst > StreamLeak.out

:: calculate the in-out stream flow and convert to ac-ft/yr
C:\ThesisCD\BIN\StrBud.exe

:: Get the updated pathline information for the y direction only
echo *** RUNNING MODPATH ***
C:\ThesisCD\BIN\ModpathV4.exe danskin.rsp

:: delete unneeded files
del fort.*
```

and UCODE.bat for the regression and residual analysis as follows:

```
@echo off
:: Run UCODE
C:\ThesisCD\BIN\Ucode_2005.exe Danskin.in Danskin

:: Run residual analysis
C:\ThesisCD\BIN\residual_analysis.exe Danskin
```

Running the Danskin Model Evaluation

To run the Danskin model evaluation using the provided batch file either click on the batch file in Microsoft Explorer or open a command prompt in the C:\ThesisCD\Calibration_DanskinFlowModel directory and type the name of the batch file. For example:

cd C:\ThesisCD\Calibration_DanskinFlowModel

UCODE.bat, or RunApps.bat

If the desired location on the respective computer is not C:\ThesisCD then the paths in each batch file will have to be adjusted accordingly. For example, the paths in batch files are the map to locations of each application as follows: **C:\ThesisCD\BIN**Factor.exe. This line from RunApps.bat above locates the application **Factore.exe** via the path, which is the highlighted portion of the line. If the location on the respective computer is different this path must be updated to have successful completion of the batch files.

Upon the execution of the batch files, applications will be invoked to perform the desired analysis. For instance, if UCODE.bat is activated, it will use the UCODE_2005.exe executable in the BIN (short for binary) directory. UCODE will read the main UCODE_2005 input file within the current directory, Danskin.in, and begin to perform the flow model evaluation (regression analysis, sensitivity analysis, or forward mode) as prescribed in the input file. Danskin.in will invoke RunApps.bat where each

application will be read in order as they appear. For instance the execution of RunApps.bat will occur as follows:

1st) The application Factor.exe will be executed. Factor.exe controls the multiplication factor on the northeastern mountain front recharge boundary conditions. The input files are: Complete.well and factor.in. Complete.well is a standard MODFLOW-2000 well package file that depicts the specified flux stresses in the basin (pumping, recharge). The file factor.in contains the multiplication factor that adjusts the northeastern mountain front recharge that is used by UCODE. Upon completion the output file is FinalStress.well.

2nd) The application WesMF2K.exe, which is the reconstruction of Danskin's original flow model from MODFLOW 96 to MODFLOW-2000, is activated. WesMF2K.exe will use the previously generated file FinalStress.well that contains the portions of the northeastern mountain front recharge adjusted by a multiplication factor as the new well package file depicting the specified fluxes.

3rd) The internal command prompt command, find, is used to extract lines that contain instances of the text string "STREAM LEAKAGE" from the main output file generated from MODFLOW, 2k.lst. The file StreamLeak.out will be generated from the find command listing the stream leakage values for each stress period the flow model ran.

4th) The application StrBud.exe will be executed. This application uses the StreamLeak.out file generated in the 3rd step as input and controls the updating of

the stream flow observations to be used during regression. The output file is StreamBudget.out which lists the year and total stream flow for that year in ac-ft/yr.

5th) Particle tracking through the aquifer is started with the application ModpathV4.exe. This executable is standard MODPATH, but recompiled to accept more observations than allowed with the default version. Particle tracking is used to simulate the path a particle will move from the supposed industrial site (source of contamination) through the aquifer for each stress period in the flow model. This information is used by UCODE to calculate residuals with respect to observed field plume locations and simulated values of the plume path.

6th) The sixth and last command is only used to remove unneeded files from the directory after all the applications are completed.

If UCODE.bat is invoked first, the execution of RunApps.bat would either cycle through parameter-estimation, sensitivity-analysis, or one forward mode iteration depending on the controls of the UCODE input file. After the completion of UCODE_2005.exe within UCODE.bat, residual analysis will be activated. Residual_Analysis.exe is a post-regression application used to perform two functions: 1) test the weighted residuals for acceptable deviations from being independent and normally distributed, and 2) calculation of statistics that can be used to identify observations that are influential in the regression. To have proper execution of the residual analysis code, UCODE_2005 has to be executed in either sensitivity-analysis or

parameter-estimation mode and the DataExchange keyword needs to be set to yes in the main UCODE_2005 input file. For further details see the UCODE_2005 documentation.

If RunApps.bat is invoked first, the 6 step cycle will run once. The control of whether or not to use an application can be accomplished using comments in the batch file, or the respective application input file. For instance, if the user decides not to run residual analysis, comment the respective line in the batch file by placing two colons in front of the line. For example:

```
:: This is a comment because of the :: and the batch file will ignore this line!
:: C:\ThesisCD\BIN\residual_analysis.exe Danskin
```

Input-Output File Explanation

The Calibration_DanskinFlowModel directory contains the needed input files and output files generated upon the completion of the applications discussed prior. The respective files are discussed as follows:

UCODE_2005 input files:

- Danksin.in: main input file for UCODE_2005 which contains the specific inputs required to control UCODE_2005. Danskin.in is created with data input blocks specific to UCODE_2005 that may read data from other files or perform a specific purpose to UCODE_2005 execution.

- File extensions of the form, .tpl: these files are template files which are used to construct the model input files used by applications that UCODE_2005 runs. For instance, 2k.lpf.tpl is used by UCODE_2005 to produce 2k.lpf, an input file required to run MODFLOW-2000.
- File extensions of the form, .ins: these files are instruction files used by UCODE_2005 to extract and read values from output files generated by the applications executed by UCODE_2005. For example, after the completion of MODFLOW-2000 the simulated heads for the observation well locations are produced. UCODE uses Heads.ins to read the simulated heads produced by MODFLOW-2000 for calculating the residuals.
- File extensions of the form, .ddt: these files represent the observation values used to calculate residuals during the execution of UCODE_2005.

UCODE_2005 output files:

- Danskin.#uout: main output file produced after the execution of UCODE_2005. This file contains an echo of the input data and selected results with respect to the mode that UCODE_2005 was executed in.
- Data exchange files produced by UCODE_2005: all files with the form Danskin._ext, where ext is extension. For instance, Danskin._ws contains the simulated equivalents and weighted residuals for graphical purposes.

- Output and data exchange files produced by residual analysis: this post processor has the following associated files: 1) Danskin.#resan which contains the summary of the residual analysis run, 2) Danskin_.rd containing the uncorrelated normal random residuals, and 3) Danskin_.rg containing the correlated normal random numbers.

MODFLOW-2000 input files:

- Danskin.nam: main input file controlling the execution of MODFLOW-2000 containing the names of the input files used and the output files to be created.
- 2k.lst: main output file produced after the execution of MODFLOW-2000. This file contains an echo of the input data and selected results with respect to the mode that MODFLOW-2000 was executed in.
- Data exchange files produced by MODFLOW-2000: some files will have the same form as UCODE_2005 extensions such as ._ext. However, the difference will be the initial name of the file. For example, **RedCalib**._ext, where RedCalib._os contains the observed and simulated head values generated from executing MODFLOW-2000.

MODPATH input files:

- Danskin.mpn: main input file controlling the execution of MODPATH particle tracking containing the names of the input files used and the output files to be created.
- summary.pth: main output file produced after the execution of MODPATH. This file contains an echo of the input data and selected results with respect to the MODPATH execution.
- Data exchange files produced by MODPATH: 1) Danskin.cbf which is cell by cell flux values saved for each stress period used to calculate the particle tracks, 2) endpoint file, which contains the final location of the particle in the aquifer, and 3) timeseries file, which contains the simulated spatial and temporal path that the particle moved through the aquifer. The timeseries file is used by UCODE_2005 to calculate residuals of the plume observation locations.

Calibration_ModifiedFlowModel

The Calibration_ModifiedFlowModel directory contains the modified flow model in MODFLOW-2000 format and the input, batch, executable, and output files used and generated during the model evaluation. The batch files used to run the applications for the modified model calibration are RunApps.bat as follows:

```
@echo off
:: Change the ungaged recharge
echo *** UPDATING THE Northeastern  Mountain Front Recharge ***
C:\ThesisCD\BIN\NEMF.exe

echo *** RUNNING MODFLOW ***
C:\ThesisCD\BIN\mf2k.exe Danskin.nam

echo *** CALCULATE THE STREAMFLOW LEAKAGE ***
find "STREAM LEAKAGE =" 2k.lst > StreamLeak.out

::calculate the in-out stream flow and convert to ac-ft/yr
C:\ThesisCD\BIN\StrBud.exe

:: Get the updated pathline information for the y direction only
echo *** RUNNING MODPATH ***
C:\ThesisCD\BIN\ModpathV4.exe danskin.rsp

:: delete some unneeded files
del fort.*
```

and UCODE.bat for the regression and residual analysis as before:

```
@echo off
:: Run UCODE
C:\ThesisCD\BIN\Ucode_2005.exe Danskin.in Danskin

:: Run residual analysis
C:\ThesisCD\BIN\residual_analysis.exe Danskin
```

Running the Modified Model Evaluation

To run the modified model, refer to the same procedure as discussed previously. Upon the execution of the batch files, applications will be invoked as discussed above to perform the desired analysis. The execution of RunApps.bat for the modified flow model is similar as above, with two newer applications as follows:

1st) The application NEMF.exe will be executed controlling the multiplication factor on the northeastern mountain front recharge, with respect to the updated boundary conditions of the modified flow model. The input files are: Pumpage_NoCN_CR.well and UNDfactor.in. Pumpage_NoCN_NR is the updated well file that has the specified flux values of the Colton-Narrows and the Crafton-Redlands Fault removed on the southeastern boundary allowing the replacement with the general head boundary. The output file is FinalStress.well which is used as the well package in the modified flow model.

2nd) The application mf2k.exe, which is standard MODFLOW-2000, is activated. mf2k.exe will use the previously generated file FinalStress.well that contains the portions of the northeastern mountain front recharge adjusted by a multiplication factor as the new well package file depicting the specified fluxes.

3rd), 4th), 5th), and 6th) steps are the same as shown above.

Input-Output File Explanation

The Calibration_ModifiedFlowModel directory contains the same needed input files and output files previously discussed. See the above description for details on the respective UCODE_2005, MODFLOW-2000, and MODPATH files.

LognormalDistribution Directory

The LognormalDistribution directory contains two subdirectories: calibration and source. The calibration subdirectory contains the input, batch, executable, and output files used and generated during the model calibration/evaluation. The source subdirectory contains the source code developed in Fortran90, the input file, and a copy of the binary executable. The batch files used to run the applications for the truncated lognormal distribution are: RunApps.bat and UCODE.bat as follows:

```
@echo off
echo **Updating the Truncated Lognormal Distribution Contamination Source **
LogNorm.exe

:: Make the MT3D run    >nul removes the screen output
echo *** RUNNING MT3D ***
C:\ThesisCD\BIN\\mt3d_big.exe RedMT3D.nam > nul

:: delete some uneeded files
del fort.*, MT3D001S.UCN, MT3D001.OBS
```

```
@echo off
:: Run UCODE
C:\ThesisCD\BIN\Ucode_2005.exe ConvertedDanskin.in Danskin

:: Run residual analysis
C:\ThesisCD\BIN\residual_analysis.exe Danskin
```

Running the Truncated Lognormal Calibration

To run the truncated lognormal model calibration, follow the same procedure as above with respect to the UCODE.bat and RunApps.bat batch files.

Upon the execution of the batch files, applications will be invoked to perform the desired analysis. RunApps.bat will execute as follows:

1st) The application LogNorm.exe will be executed (Figure A.1). Two output files are produced: 1) MASSCHECK.OUT listing the year, mass for that year, and a summation of the total mass of the distribution, and 2) BLD91_LN.ssm, which is a sink-source mixing file used by the transport model to simulate the TCE source.

2nd) The MT3DMS transport application mt3d_big.exe is invoked. This executable is exactly the same as standard MT3DMS, but only recompiled to accept a larger amount of concentration observations and simulates the transport of TCE within ground water using the previously created BLD91_LN.ssm file.

If UCODE.bat is invoked first, as discussed above, the execution of RunApps.bat would either cycle through parameter-estimation, sensitivity-analysis, or one forward mode iteration depending on the controls of the UCODE input file.

Input-Output File Explanation

The calibration subdirectory of the LognormalDistribution directory contains the needed input files and output files generated upon the completion of the applications discussed prior. Note, the input-output file explanation remains the same for each of the alternative conceptual transport models

UCODE_2005 input files:

- ConvetedDanksin.in: main input file for UCODE_2005.
- File extensions of the form, .tpl: these are template files discussed above
- File extensions of the form, .ins: these are instruction files discussed above.
- File extensions of the form, .ddt: these are observation values discussed above.

UCODE_2005 output files: (discussed above)

MT3DMS input files:

- RedMT3D.nam: main input file controlling the execution of MT3DMS. Contains the names of the input files used and the output files to be created.
- Red.m3d: main output file produced after the execution of MT3DMS. This file contains an echo of the input data and selected results with respect to the mode that MT3DMS was executed in.
- Data exchange files produced by MT3DMS: the main file for post-processing is MT3D001.UCN which is a binary output file containing the simulated concentration data for each stress period.

Post-Processing

Note: post processing remains the same for each of the alternative conceptual transport models. Two batch files, Grid.bat and FileConvert.bat, are included that are used for post processing after the transport simulation is complete to generate contour plume maps:

```
@echo off
rem Batch file to create surfer grids of Redlands TCE output
rem delete unwanted files (rem is another form of commenting in a batch file)
del MT3D001S.UCN MT3D001S.OBS
C:\ThesisCD\BIN\pm.exe
```

```
@echo off
:: Convert the file from lbs/cu.ft to ppb
C:\ThesisCD\BIN\convert.exe
```

The batch file, Grid.bat is used to remove unneeded files and invoke a post processing application that is included with MT3DMS for contouring concentration data, PostMT3D|MOFLOW, or pm.exe. For this project pm.exe reads both the binary file MT3D001.UCN and the grid configuration file Red.cnf produced by MT3DMS.

To execute Grid.bat properly the following must be done sequentially:

1st) Type Grid.bat in the command prompt, or double click within the directory and follow the input instructions accordingly.

2nd) The program will ask for the name of the unformatted concentration file, type MT3D001.UCN

3rd) The program will ask for the style of the unformatted file, type 2 for binary

4th) The program will ask for the model grid configuration file, type Red.cnf

5th) The program will ask if you wish to offset the coordinates, type n

6th) The program will ask for the total elapsed time at which a contour map is needed, type -1 for the final step. The option for other times is also allowed.

7th) The program will ask for the starting column, row, and layer, type 1,1,1

8th) The program will ask for the ending column, row, and layer, type 184,118,1

9th) The program will ask for a name to be given to the file that is about to be generated. For this response type a desired name. However, add the extension with the name as pm.exe does not do this, i.e., gridfile**.grd**. Throughout this work surfer is used for contouring purposes and to make the final post processing step complete you must use the .grd format extension.

10th) The program asks for the format of the data file, type 1 for surfer grid format.

The batch file, FileConvert.bat is used to recreate the surfer grid file produced from Grid.bat such that the final surfer grid file will have concentrations in parts per billion (ppb) instead of lbs/ft^3. FileConvert.bat invokes the application convert.exe. The input file is requested upon execution and is with respect to the chosen file name after the completion of Grid.bat. The output file name is also requested and will be in the form: **RequestedFileName**.grd, where RequestedFileName is selected by the user. The user does not have to include the .grd extension as it is automatically added.

NormalDistribution Directory

The NormalDistribution directory contains the same directory structure and descriptions as the LognormalDistribution. The batch files used to run the applications for the truncated normal distribution are the same except that RunApps.bat has a different executable to produce the truncated normal distribution:

```
@echo off
echo **Updating the Truncated Normal Distribution Contamination Source **
NormDist.exe

:: Make the MT3D run    >nul removes the screen output
echo *** RUNNING MT3D ***
C:\ThesisCD\BIN\\mt3d_big.exe RedMT3D.nam > nul

:: delete some uneeded files
del fort.*, MT3D001S.UCN, MT3D001.OBS
```

Running the Truncated Normal Calibration

To run the truncated lognormal model calibration, follow the same procedure as above with respect to the UCODE.bat and RunApps.bat batch files.

Upon the execution of the batch files, applications will be invoked to perform the desired analysis. RunApps.bat will execute as described above:

1st) The application NormDist.exe will be executed (Figure A.1). Two output files are produced: 1) MASSCHECK.OUT described above, and 2) BLD91_ND.ssm to simulate a truncated normal TCE source.

2nd) Same as above, but using the previously created BLD91_ND.ssm file.

StakeHolder Directory

The StakeHolder directory contains the same directory structure and descriptions as the alternative source function directories. The batch files used to run the applications for the stake holder function are the same except that RunApps.bat has a different executable to produce the stake holder distribution:

```
@echo off
echo *** Updating Stake Holder Mass Distribution ***
StakeHolder.exe

:: Make the MT3D run
echo *** RUNNING MT3D ***
C:\ThesisCD\BIN\mt3d_big.exe RedMT3D.nam > nul

:: delete some uneeded files
del MT3D001.OBS
```

Running the Stake Holder Calibration

To run the stake holder model calibration, follow the same procedure as above with respect to the UCODE.bat and RunApps.bat batch files.

Upon the execution of the batch files, applications will be invoked to perform the desired analysis. RunApps.bat will execute as described above:

1st) The application StakeHolder.exe will be executed (Figure A.3). Two output files are produced: 1) MASSCHECK.OUT described above, and 2) BLD91_SH.ssm to simulate the stake holder distribution of a TCE source.

2nd) Same as above, but using the previously created BLD91_SH.ssm file.

StepFunction Directory

The StepFunction directory contains the same directory structure and descriptions as the other alternative source function directories. The batch files used to run the applications for the step function are the same except that RunApps.bat has a different executable to produce the step function distribution:

```
@echo off
echo *** Updating the Step Function ***
srcdis.exe

:: Make the MT3D run
echo *** RUNNING MT3D ***
C:\ThesisCD\BIN\mt3d_big.exe RedMT3D.nam > nul

:: delete some uneeded files
del MT3D001S.UCN, MT3D001.OBS
```

Running the Step Funciton Calibration

To run the step function model calibration, follow the same procedure as above with respect to the UCODE.bat and RunApps.bat batch files.

Upon the execution of the batch files, applications will be invoked to perform the desired analysis. RunApps.bat will execute as described above:

1st) The application srcdis.exe will be executed (Figure A.2). Two output files are produced: 1) MASSCHECK.OUT described above, and 2) BLD91_cont.ssm to simulate the step function distribution of a TCE source.

2nd) Same as above, but using the previously created BLD91_cont.ssm file.